Circulation Research

ORIGINAL RESEARCH

Increased Ca^{2+} Transient Underlies RyR2-Related Left Ventricular Noncompaction

Mingke Ni, Yanhui Li, Jinhong Wei, Zhenpeng Song, Hui Wang, Jinjing Yao, Yong-Xiang Chen, Darrell Belke, John Paul Estillore, Ruiwu Wang, Alexander Vallmitjana, Raul Benitez, Leif Hove-Madsen, Wei Feng, Ju Chen, Thomas M. Roston, Shubhayan Sanatani, Anna Lehman, S.R. Wayne Chen

BACKGROUND: A loss-of-function cardiac ryanodine receptor (RyR2) mutation, I4855M$^{+/-}$, has recently been linked to a new cardiac disorder termed RyR2 Ca^{2+} release deficiency syndrome (CRDS) as well as left ventricular noncompaction (LVNC). The mechanism by which RyR2 loss-of-function causes CRDS has been extensively studied, but the mechanism underlying RyR2 loss-of-function-associated LVNC is unknown. Here, we determined the impact of a CRDS-LVNC-associated RyR2-I4855M$^{+/-}$ loss-of-function mutation on cardiac structure and function.

METHODS: We generated a mouse model expressing the CRDS-LVNC-associated RyR2-I4855M$^{+/-}$ mutation. Histological analysis, echocardiography, ECG recording, and intact heart Ca^{2+} imaging were performed to characterize the structural and functional consequences of the RyR2-I4855M$^{+/-}$ mutation.

RESULTS: As in humans, RyR2-I4855M$^{+/-}$ mice displayed LVNC characterized by cardiac hypertrabeculation and noncompaction. RyR2-I4855M$^{+/-}$ mice were highly susceptible to electrical stimulation–induced ventricular arrhythmias but protected from stress-induced ventricular arrhythmias. Unexpectedly, the RyR2-I4855M$^{+/-}$ mutation increased the peak Ca^{2+} transient but did not alter the L-type Ca^{2+} current, suggesting an increase in Ca^{2+}-induced Ca^{2+} release gain. The RyR2-I4855M$^{+/-}$ mutation abolished sarcoplasmic reticulum store overload–induced Ca^{2+} release or Ca^{2+} leak, elevated sarcoplasmic reticulum Ca^{2+} load, prolonged Ca^{2+} transient decay, and elevated end-diastolic Ca^{2+} level upon rapid pacing. Immunoblotting revealed increased level of phosphorylated CaMKII (Ca^{2+}-calmodulin dependent protein kinases II) but unchanged levels of CaMKII, calcineurin, and other Ca^{2+} handling proteins in the RyR2-I4855M$^{+/-}$ mutant compared with wild type.

CONCLUSIONS: The RyR2-I4855M$^{+/-}$ mutant mice represent the first RyR2-associated LVNC animal model that recapitulates the CRDS-LVNC overlapping phenotype in humans. The RyR2-I4855M$^{+/-}$ mutation increases the peak Ca^{2+} transient by increasing the Ca^{2+}-induced Ca^{2+} release gain and the end-diastolic Ca^{2+} level by prolonging Ca^{2+} transient decay. Our data suggest that the increased peak-systolic and end-diastolic Ca^{2+} levels may underlie RyR2-associated LVNC.

GRAPHIC ABSTRACT: A graphic abstract is available for this article.

Key Words: cardiac ryanodine receptor ■ cardiomyopathies ■ left ventricular noncompaction ■ sarcoplasmic reticulum ■ ventricular tachyarrhythmia

The cardiac ryanodine receptor (RyR2) is an intracellular Ca^{2+} channel that governs the release of Ca^{2+} from the sarcoplasmic reticulum (SR) in heart muscle cells. RyR2-mediated SR Ca^{2+} release constitutes an essential step in the process of Ca^{2+}-induced Ca^{2+} release (CICR) that underlies excitation-contraction coupling in the heart.[1–3] Thus, aberrant RyR2 function would be detrimental and pathogenic. Indeed, RyR2 gain-of-function (GOF) mutations cause catecholaminergic polymorphic ventricular tachycardia (CPVT), a hereditary cardiac disorder characterized by syncope, malignant ventricular arrhythmias and sudden cardiac death in the absence of structural heart disease.[4–8] Extensive functional studies over the past 2 decades have greatly advanced our

Correspondence to: S.R. Wayne Chen, 3330 Hospital Dr N.W., Calgary, Alberta, Canada T2N 4N1. Email swchen@ucalgary.ca
Supplemental Material is available at https://www.ahajournals.org/doi/suppl/10.1161/CIRCRESAHA.123.322504.
For Sources of Funding and Disclosures, see page XXX.

Circulation Research is available at www.ahajournals.org/journal/res

Novelty and Significance

What Is Known?

- Human cardiac ryanodine receptor (RyR2)-I4855M$^{+/-}$ loss-of-function (LOF) mutant carriers present with left ventricular noncompaction (LVNC) and Ca^{2+} release deficiency syndrome (CRDS) overlapping phenotype.
- Recent studies have revealed important insights into the arrhythmogenic mechanism of CRDS, but the mechanism by which RyR2 I4855M$^{+/-}$ LOF mutation causes LVNC is largely unknown.
- There is currently no animal model of RyR2-associated LVNC.

What New Information Does This Article Contribute?

- A novel mouse model harboring the LVNC-associated RyR2 LOF mutation I4855M$^{+/-}$ recapitulates the LVNC and CRDS overlapping phenotype in humans.
- The LVNC RyR2 I4855M$^{+/-}$ mutation enhances the peak Ca^{2+} transient by increasing the Ca^{2+}-induced Ca^{2+} release gain and the sarcoplasmic reticulum (SR) Ca^{2+} load.
- Increased peak systolic Ca^{2+} transient is an important determinant of RyR2-associated LVNC.

Human cardiac ryanodine receptor (RyR2) mutations have been associated with ventricular arrhythmias and left ventricular noncompaction (LVNC). The mechanisms underlying RyR2-associated VAs have been extensively investigated over the past more than 2 decades. However, little is known about the mechanism by which RyR2 mutations cause LVNC. To assess the role of RyR2 in LVNC, we generated the first RyR2 LVNC mouse model harboring the LVNC-associated RyR2 I4855M$^{+/-}$ LOF mutation. Here, we demonstrated that the RyR2 I4855M$^{+/-}$ mouse model recapitulates the ventricular arrhythmia and LVNC overlapping phenotype in humans. Mechanistically, we found that the RyR2 I4855M$^{+/-}$ LVNC mutation increased the amplitude of systolic Ca^{2+} transients, likely resulting from the enhanced Ca^{2+}-induced Ca^{2+} release gain and elevated sarcoplasmic reticulum Ca^{2+} load due to diminished sarcoplasmic reticulum Ca^{2+} leak. The RyR2 LVNC mutation also elevated end-diastolic Ca^{2+} level as a result of prolonged Ca^{2+} transient decay due in part to the elevated sarcoplasmic reticulum Ca^{2+} content. Furthermore, the level of phosphorylated CaMKII (Ca^{2+}-calmodulin dependent protein kinases II) was increased in the RyR2 LVNC I4855M$^{+/-}$ mutant hearts compared with WT hearts. These findings suggest that increased peak-systolic Ca^{2+} transient and end-diastolic Ca^{2+} level are important determinants of RyR2 associated LVNC. Thus, targeting the peak-systolic and end-diastolic Ca^{2+} levels may offer a therapeutic strategy for RyR2-associated LVNC.

Nonstandard Abbreviations and Acronyms

CaM	calmodulin
CaMKII	Ca^{2+}/CaM-dependent protein kinase II
CICR	Ca^{2+}-induced Ca^{2+} release
CPVT	catecholaminergic polymorphic ventricular tachycardia
CRDS	Ca^{2+} release deficiency syndrome
GOF	gain-of-function
LOF	loss-of-function
LVNC	left ventricular noncompaction
NCX	Na^{+}/Ca^{2+} exchanger
PLB	phospholamban
RyR2	cardiac ryanodine receptor
SERCA2a	Sarco/endoplasmic reticulum Ca^{2+} ATPase 2a
SR	sarcoplasmic reticulum
VA	ventricular arrhythmia
WT	wildtype

understanding of the disease mechanism of CPVT. It is now well established that aberrant RyR2 GOF increases the propensity for spontaneous Ca^{2+} release in the form of Ca^{2+} waves during SR Ca^{2+} overload.[7,9] These store overload–induced Ca^{2+} waves can activate the electrogenic Na^{+}/Ca^{2+} exchanger and evoke delayed afterdepolarizations (DADs), which in turn can lead to triggered activity and malignant ventricular arrhythmias.[7,9]

In addition to CPVT-associated RyR2 GOF mutations, there are also disease-associated loss-of-function (LOF) RyR2 mutations.[10–16] These RyR2 LOF mutations have recently been linked to a new cardiac arrhythmia disorder, termed RyR2 Ca^{2+} release deficiency syndrome (CRDS).[16] CRDS is characterized by malignant ventricular arrhythmias and sudden cardiac death but does not exhibit typical CPVT phenotypes.[16] Unlike typical CPVT patients who display stress-induced bidirectional and polymorphic ventricular tachycardias during exercise stress testing, CRDS patients typically present with normal clinical testing including negative exercise stress testing for CPVT.[16] Furthermore, the underlying disease mechanism of CRDS is also different from that of CPVT.

Contrasting to CPVT RyR2 GOF mutations, RyR2 LOF mutations suppress the occurrence of spontaneous Ca^{2+} waves during SR Ca^{2+} overload, Ca^{2+} wave-evoked DADs, and triggered activity, but increase the propensity for Ca^{2+} alternans, early-afterdepolarizations (EADs)[13] and reentrant arrhythmias.[16] Therefore, RyR2 mutations can cause distinct cardiac arrhythmia disorders depending on their impact on RyR2 function.

A large number of disease related RyR2 mutations have been identified to date. Most of these RyR2 mutations are associated with cardiac arrhythmias and sudden death without structural heart disease. However, there are some RyR2 mutant carriers who present with cardiomyopathies as well as cardiac arrhythmias.[6,7,17–23] For instance, several unrelated families with an in-frame deletion of exon-3 in the *RYR2* gene presented with an expanding spectrum of phenotypes, including left ventricular noncompaction cardiomyopathy (LVNC) as well as CPVT.[6,24–30] In vitro functional characterization revealed that the exon-3 deletion reduced the threshold for store overload–induced spontaneous Ca^{2+} release,[31] which may account for the increased propensity for stress-induced ventricular arrhythmias (VAs; ie, CPVT). Interestingly, the exon-3 deletion also markedly reduced the threshold at which spontaneous Ca^{2+} release terminates.[31] Furthermore, it was recently reported that 3 patients with the RyR2 mutation R169Q also presented with LVNC as well as CPVT.[32] As with the exon-3 deletion, in vitro functional analyses revealed that the RyR2-R169Q mutation reduced both the activation and termination thresholds for store overload–induced spontaneous Ca^{2+} release.[32] Therefore, LVNC can coexist with CPVT that is associated with RyR2 GOF mutations.

We have previously shown that human RyR2-I4855M$^{+/-}$ LOF mutant carriers presented with LVNC as well as a history of ventricular arrhythmias and sudden death, a phenotype consistent with CRDS but distinct from CPVT.[15,33] This observation suggests that LVNC can also coexist with CRDS that is associated with RyR2 LOF mutations. Although our recent work has revealed important insights into the arrhythmogenic mechanism of CRDS, little is known about the mechanism by which RyR2 I4855M$^{+/-}$ LOF mutation results in LVNC. There is currently no animal model of LVNC associated with RyR2 mutations. To this end, in the present study, we generated a novel knock-in mouse model expressing the RyR2-I4855M$^{+/-}$ LOF mutation. We found that, as in humans, the RyR2-I4855M$^{+/-}$ LOF mutant mice exhibited LVNC. Interestingly, the I4855M$^{+/-}$ LOF mutant mice also displayed left ventricular hypertrophic cardiomyopathy and left ventricular fibrosis. Furthermore, the I4855M$^{+/-}$ mice lack stress-induced ventricular arrhythmias but were highly susceptible to programed electrical stimulation–induced ventricular arrhythmias, which is consistent with the CRDS phenotype. Thus, our RyR2-I4855M$^{+/-}$ LOF mutant mouse model recapitulates the CRDS-LVNC overlapping phenotype in humans. Mechanistically, we found that the RyR2-I4855M$^{+/-}$ mutation diminished store-overload induced Ca^{2+} release or spontaneous SR Ca^{2+} release, increased SR Ca^{2+} content, and elevated the peak amplitude of depolarization-induced Ca^{2+} transients. Furthermore, the I4855M$^{+/-}$ mutation prolonged Ca^{2+} transient decay and increased the end-diastolic intracellular Ca^{2+} level upon rapid pacing. Given the well-established link between increased peak-systolic and end-diastolic Ca^{2+} levels and cardiac remodeling in cardiomyopathies,[2,34–45] elevated peak-systolic and end-diastolic Ca^{2+} levels may underlie RyR2-I4855M$^{+/-}$ associated LVNC.

METHODS

Data Availability

All data and supporting materials associated with this study are available in the article and the Supplemental Material. The intact heart Ca^{2+} imaging analysis tool written in MATLAB is available upon request. Please contact R. Benitez (raul.benitez@upc.edu) for Ca^{2+} imaging analysis tool.

General Methods

To investigate the cellular and molecular mechanisms underlying RyR2-related LVNC, we generated a knock-in mouse model expressing the LVNC-associated RyR2-I4855M$^{+/-}$ LOF mutation using homologous recombination in embryonic stem cells. Cardiac structure was assessed using hematoxylin and eosin staining, Picrosirius red staining, and echocardiographic analysis. Surface ECG and intracardiac ECG recordings were applied to determine the susceptibility to stress-induced and programed electrical stimulation triggered ventricular arrhythmias. Confocal in situ Ca^{2+} imaging was carried out to assess the impact of the RyR2-I4855M$^{+/-}$ mutation on the properties of membrane depolarization-induced Ca^{2+} release and store-overload induced Ca^{2+} release in the form of spontaneous Ca^{2+} waves in intact working hearts. Detailed methods are provided in the Supplemental Material.

RESULTS

RyR2-I4855M$^{+/-}$ Mutant Mice Display LVNC

The RyR2-I4855M LOF mutation was identified in patients presenting with LVNC and CRDS.[15,16,33] To assess the potential link between RyR2-I4855M LOF mutation and LVNC, we generated a novel mouse model expressing the RyR2-I4855M mutation (Figure S1). As in humans, only heterozygous RyR2-I4855M mutant mice (RyR2-I4855M$^{+/-}$), but no homozygous mutant mice were observed, suggesting that homozygous RyR2-I4855M $^{+/+}$ mutation is embryonically lethal. We then performed hemotoxylin and eosin (H&E) staining of heart slices from RyR2 wild-type (WT) and heterozygous I4855M$^{+/-}$ mutant mice (both males and females; Figure 1A through 1D). We assessed the ratio of the

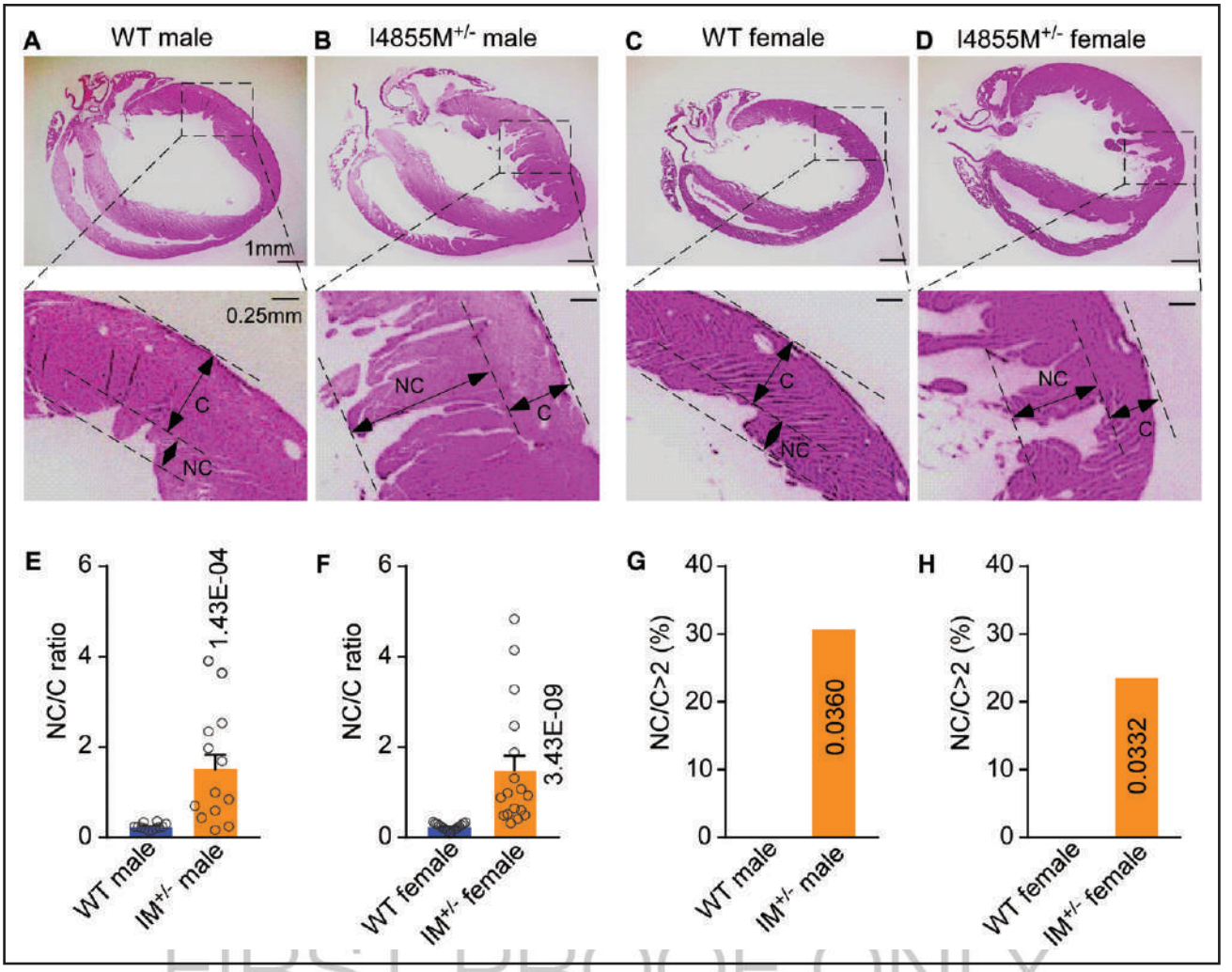

Figure 1. RyR2-I4855M$^{+/-}$ mutant mice display left ventricular noncompaction (LVNC).
Histological analysis (H&E staining) of heart sections from RyR2-WT male (**A**) and female (**C**) and RyR2-I4855M$^{+/-}$ mutant male (**B**) and female (**D**) mice. RyR2-WT ventricular walls show compacted myocardium (enlarged areas in **A** and **C**), whereas RyR2-I4855M$^{+/-}$ mutant ventricular walls show large trabeculae (enlarged areas in **B** and **D**). The noncompaction layer (NC)/compaction (C) ratios in male (**E**) and female (**F**) RyR2 WT and I4855M$^{+/-}$ mutant hearts. The percentage (%) of male (**G**) and female (**H**) RyR2 WT and I4855M$^{+/-}$ mutant hearts presenting with NC/C ratios greater than 2. Data are Mean±SEM from WT mice (n=12 males and 17 females) and I4855M$^{+/-}$ mutant mice (n=13 males and 17 females) with the *P* values indicated for I4855M$^{+/-}$ vs WT (Mann-Whitney *U* test (**E** and **F**) and χ^2 test (**G** and **H**).

noncompaction (NC) ventricular layer over the compacted (C) ventricular layer (NC/C), a widely used criteria for diagnosis of LVNC, which should have a NC/C ratio >2.0.[46] We found that the average NC/C ratio of the RyR2-I4855M$^{+/-}$ mutant hearts was markedly increased compared with that of the WT hearts from both males and females (Figure 1E and 1F). Importantly, a significant fraction (~25-30%) of the RyR2-I4855M$^{+/-}$ mutant hearts (both males and females), but none of the WT hearts displayed trabeculation with a NC/C ratio >2.0 (Figure 1G and 1H). Thus, the RyR2-I4855M$^{+/-}$ mutant mouse model recapitulates LVNC phenotype observed in human RyR2-I4855M$^{+/-}$ mutant carriers.

We have recently reported a mouse model expressing the RyR2-D4646A$^{+/-}$ LOF mutation that is associated with CRDS without cardiomyopathy in humans.[16] To assess whether LVNC is present in this CRDS mouse model, we determined the NC/C ratio in the RyR2-WT and RyR2-D4646A$^{+/-}$ mutant hearts. We found that there was no significant difference in the NC/C ratio between RyR2-WT and RyR2-D4646A$^{+/-}$ hearts (Figure S2). Like RyR2-WT, but different from the RyR2-I4855M$^{+/-}$ mutant hearts, none of the RyR2-D4646A$^{+/-}$ mutant hearts displayed trabeculation with a NC/C ratio >2.0 (Figure S2). Therefore, as in human patients harboring the RyR2-D4646A$^{+/-}$ mutation, the CRDS RyR2-D4646A$^{+/-}$ mouse model does not display LVNC.

RyR2-I4855M$^{+/-}$ Mutant Mice Show Left Ventricular Hypertrophy and Fibrosis

LVNC is often associated with other cardiomyopathies, such as hypertrophic cardiomyopathy.[47–52] To assess the potential association of LVNC with hypertrophy in the

RyR2-I4855M$^{+/-}$ mutant mice, we measured the heart/body weight ratios of RyR2 WT and I4855M$^{+/-}$ mutant mice. We found that RyR2-I4855M$^{+/-}$ mutant males displayed a significantly higher heart/body weight ratio compared with RyR2 WT males, whereas the heart/body weight ratios were not significantly different between RyR2 WT and I4855M$^{+/-}$ mutant females (Figure 2A through 2F). We also found that the cell size in the male I4855M$^{+/-}$ mutant hearts was significantly greater than that in the male WT hearts, whereas female WT and I4855M$^{+/-}$ mutant hearts showed similar cell sizes (Figure 2G and 2H).

To further investigate this hypertrophic phenotype, we performed echocardiography on RyR2 WT or I4855M$^{+/-}$ mutant mice. We found that male RyR2-I4855M$^{+/-}$ mutant mice displayed reduced LV diameter, increased thickness of the LV anterior and posterior walls, and increased left ventricular mass (Figure 3). Interestingly, despite the hypertrophic phenotype, the RyR2-I4855M$^{+/-}$ mutation increased the ejection fraction and fractional shortening, but decreased heart rate in male mice (Figure 3). Furthermore, the isovolumic relaxation time was significantly increased in male RyR2-I4855M$^{+/-}$ mutant mice compared with male WT mice, suggesting that the diastolic function is also impaired in male RyR2-I4855M$^{+/-}$ mutant hearts. Collectively, these data reveal that male RyR2-I4855M$^{+/-}$ mutant mice are associated with both LVNC and left ventricular hypertrophy. Note that there were no male I4855M$^{+/-}$ mutant carriers in the family. Hence, it is unknown whether the I4855M$^{+/-}$ mutation also causes left ventricular hypertrophy in human male RyR2-I4855M$^{+/-}$ mutant carriers.

Consistent with the histological analysis, echocardiography also revealed that female RyR2-I4855M$^{+/-}$ mutant mice did not have overt left ventricular hypertrophic phenotype as evidenced by the unchanged LV diameter or LV wall thickness in RyR2-I4855M$^{+/-}$ mutant females compared with those in WT females (Figure S3). This is also consistent with the clinical presentations of human female RyR2-I4855M$^{+/-}$ mutant carriers who displayed LVNC but no hypertrophic cardiomyopathy.[15,33] Interestingly, however, both male and female RyR2-I4855M$^{+/-}$ mutant mice showed significantly increased left ventricular mass, increased isovolumic relaxation time, and reduced heart rate (Figure 3; Figure S3). Moreover, both male and female RyR2-I4855M$^{+/-}$ mutant mice displayed left atrium hypertrophy as evidenced by the significantly increased area of the left atrium compared with WT mice (Figure S4). These observations indicate that female RyR2-I4855M$^{+/-}$ mutant mice also exhibited some cardiac structural and functional defects.

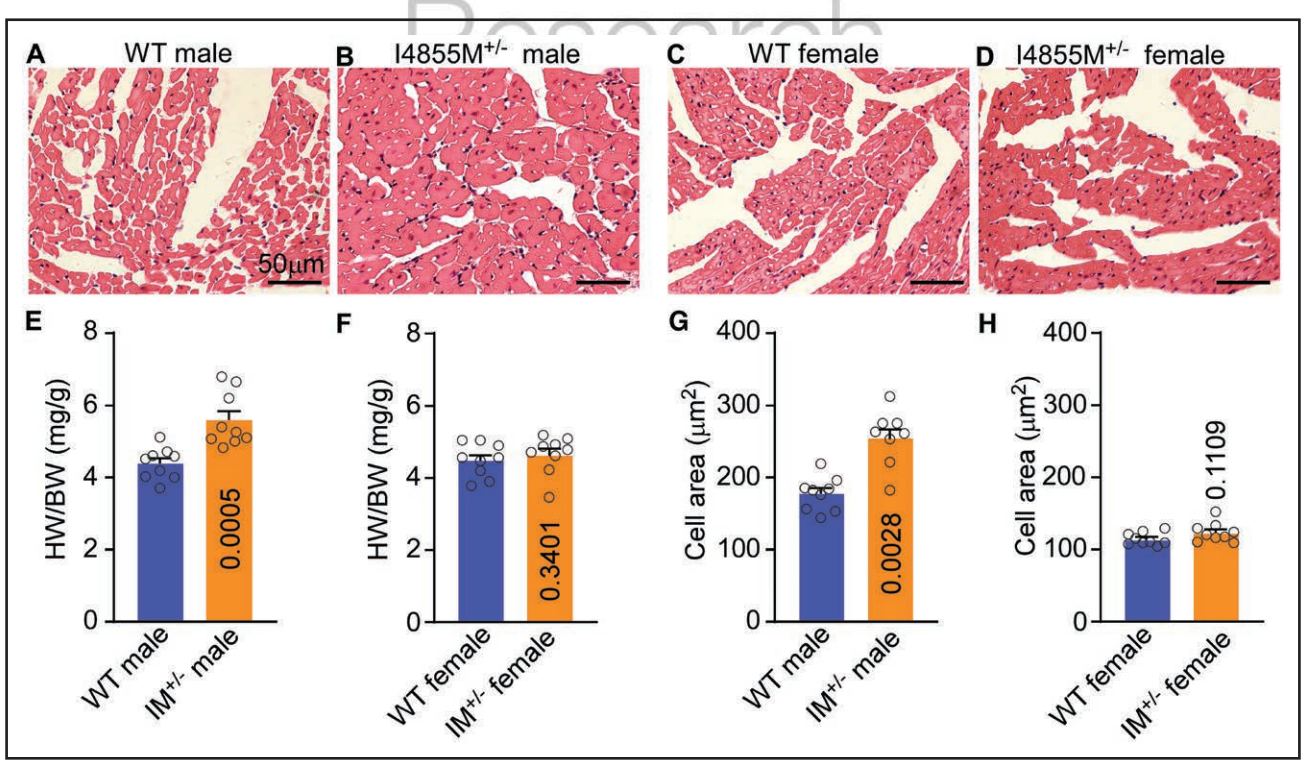

Figure 2. The RyR2-I4855M$^{+/-}$ mutation increases heart weight/body weight ratio in male but not female mice.
H&E staining of heart sections from RyR2-WT male (**A**) and female (**C**) and RyR2-I4855M$^{+/-}$ mutant male (**B**) and female (**D**) mice. The heart weight to body weight ratio (HW/BW, mg/g) in male (**E**) and female (**F**) RyR2-WT and I4855M$^{+/-}$ mutant mice. Data shown are mean±SEM from WT mice (n=9 males and 9 females) and RyR2-I4855M$^{+/-}$ mutant mice (n=9 males and 9 females; Student *t* test vs WT). The cell area in male (**G**) and female (**H**) RyR2-WT and I4855M$^{+/-}$ mutant mice. Data are mean±SEM from RyR2-WT mice (n=9 males and 9 females) and RyR2-I4855M mutant mice (n=8 males and 9 females) with the *P* values indicated for I4855M$^{+/-}$ vs WT (Mann-Whitney *U* test).

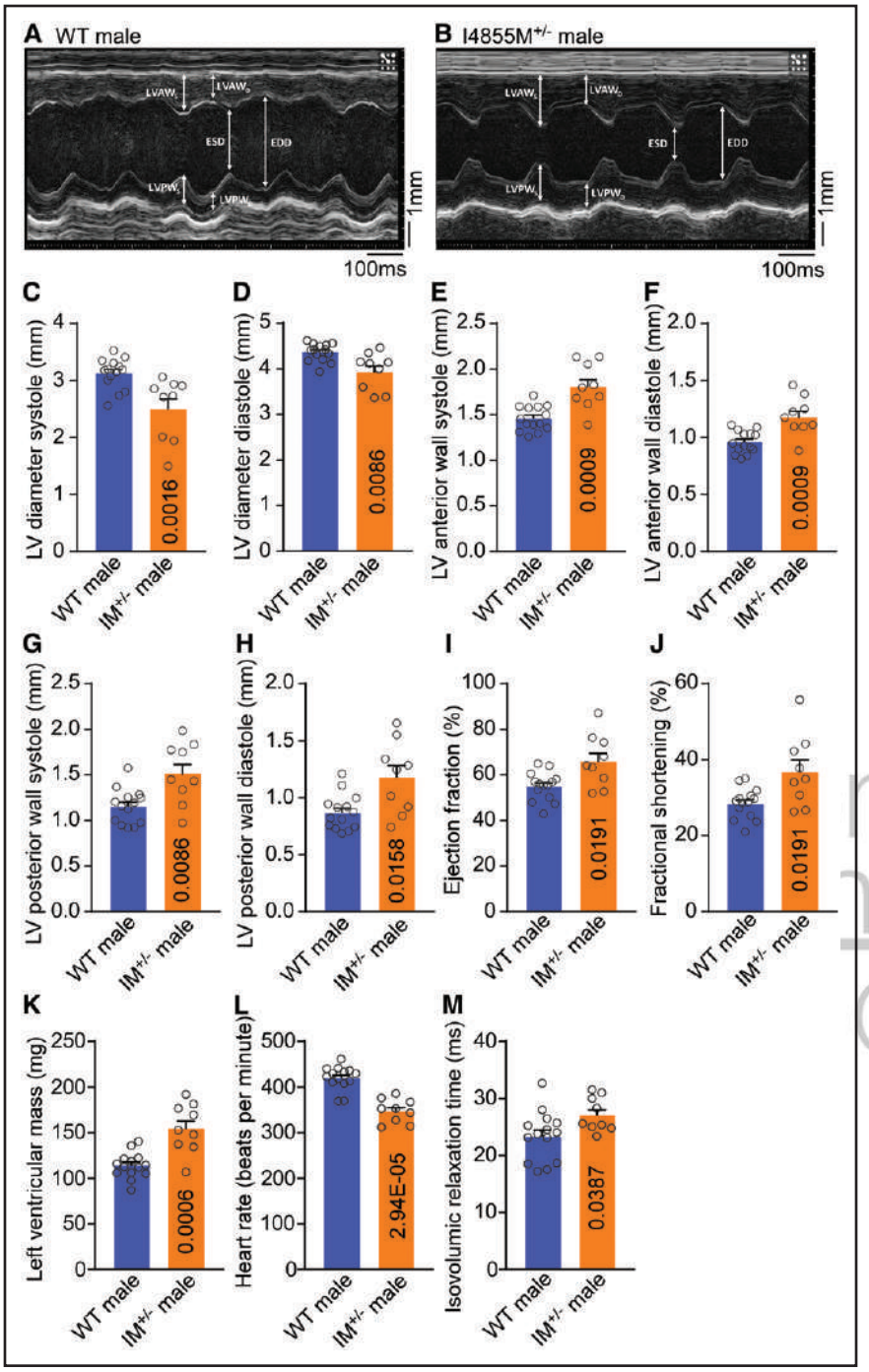

Figure 3. The RyR2-I4855M$^{+/-}$ mutation causes left ventricular (LV) hypertrophy in male mice. Representative M-mode echocardiographs from male RyR2-WT mice (**A**) and male RyR2-I4855M$^{+/-}$ mutant mice (**B**; scale bars, 100 ms, 1 mm). Echocardiographic parameters, LV diameter systole (**C**); LV diameter diastole (**D**); LV anterior wall thickness systole (**E**); LV anterior wall thickness diastole (**F**); LV posterior wall thickness systole (**G**); LV posterior wall thickness diastole (**H**); LV ejection fraction (**I**); LV fractional shortening (**J**); left ventricular mass (**K**); heart rate (**L**); and isovolumic relaxation time (**M**) are compared between male RyR2-WT and male RyR2-I4855M$^{+/-}$ mutant mice. Data are mean±SEM from WT (n=14 male mice) and RyR2-I4855M$^{+/-}$ mutant (n=9 male mice) with the *P* values indicated for I4855M$^{+/-}$ vs WT (Mann-Whitney *U* test).

Hypertrophic cardiomyopathy is often associated with fibrosis.[53,54] To determine whether the RyR2-I4855M$^{+/-}$ mutation is also associated with collagen remodeling, we performed picrosirius red staining of heart slices from male and female RyR2 WT and I4855M$^{+/-}$ mutant mice. We found that male, but not female RyR2-I4855M$^{+/-}$ mutant hearts exhibited increased collagen staining compared with male and female WT hearts, respectively (Figure S5). Taken together, our data indicate that the RyR2-I4855M$^{+/-}$ mutation can lead to LVNC and left ventricular hypertrophy and fibrosis in mice.

RyR2-I4855M$^{+/-}$ Mutant Mice Are Protected From Stress-Induced CPVT

In addition to the LVNC phenotype, patients harboring the RyR2-I4855M$^{+/-}$ mutation also displayed CRDS phenotype with negative exercise stress testing for CPVT.[15,16,33] To assess whether RyR2-I4855M$^{+/-}$ mutant mice also have this CRDS phenotype, we tested the susceptibility of the RyR2-I4855M$^{+/-}$ mutant mice (both males and females) to stress-induced ventricular arrhythmias (ie, CPVT). A mixture of low doses of caffeine (120 mg/kg) and epinephrine (1.6 mg/kg) has commonly been

used as pharmacological triggers for CPVT in animal studies.[55–59] We have previously shown that the CRDS RyR2-D4646A$^{+/-}$ LOF mutant mouse model is resistant to CPVT evoked by high doses of caffeine (150 mg/kg) and epinephrine (3.0 mg/kg).[16] Similarly, we found that the same high doses of caffeine and epinephrine did not induce ventricular arrhythmias in male or female RyR2-I4855M$^{+/-}$ mutant mice (Figure 4). In fact, the RyR2-I4855M$^{+/-}$ mutation protected against caffeine/epinephrine-provoked ventricular arrhythmias compared with WT (Figure 4). This is opposite to the action of typical CPVT-promoting RyR2 GOF mutations[7] but consistent with the negative CPVT observed in human RyR2-I4855M$^{+/-}$ mutant carriers.[15,33]

RyR2-I4855M$^{+/-}$ Mutant Mice Are Highly Susceptible to LBLPS-Induced Ventricular Arrhythmias

We have recently shown that a mouse model of CRDS and human CRDS patients are susceptible to programed electrical stimulation-induced VAs.[16] To determine whether the RyR2-I4855M$^{+/-}$ mutant mice are also susceptible to programed electrical stimulation-induced VAs, we performed in vivo intracardiac electrical stimulations and electrogram recordings to assess the VA inducibility of several stimulation protocols, including (1) a burst pacing, (2) a long pause, (3) a short-coupled premature ventricular stimulation (S1S2 stimulation), and (4) a 3-component protocol consisting of a long burst, a long pause, and a short-coupled extra-stimulus (LBLPS). As shown in Figure 5, none of the 3 commonly used stimulation protocols (a long burst, a long burst+a long pause, and S1S2 stimulation) reliably induced VAs in male or female RyR2-I4855M$^{+/-}$ mutant mice (Figure 5A through 5F). On the other hand, the LBLPS stimulation protocol, known to induce VA in CRDS, consistently and robustly provoked VAs in the RyR2-I4855M$^{+/-}$ mutant, but not in WT mice (both males and females; Figure 5G through 5K). Thus, the RyR2-I4855M$^{+/-}$ mutation increases the susceptibility to LBLPS-induced VAs in mice.

Isolated Intact RyR2-I4855M$^{+/-}$ Mutant Hearts Are Prone to LBLPS-Induced VA-Like Irregular Ca^{2+} Transients

To determine whether isolated hearts are also susceptible to LBLPS-induced VAs, we performed in situ confocal Ca^{2+} imaging of ventricular myocytes in the epicardium of isolated intact hearts from RyR2-WT and

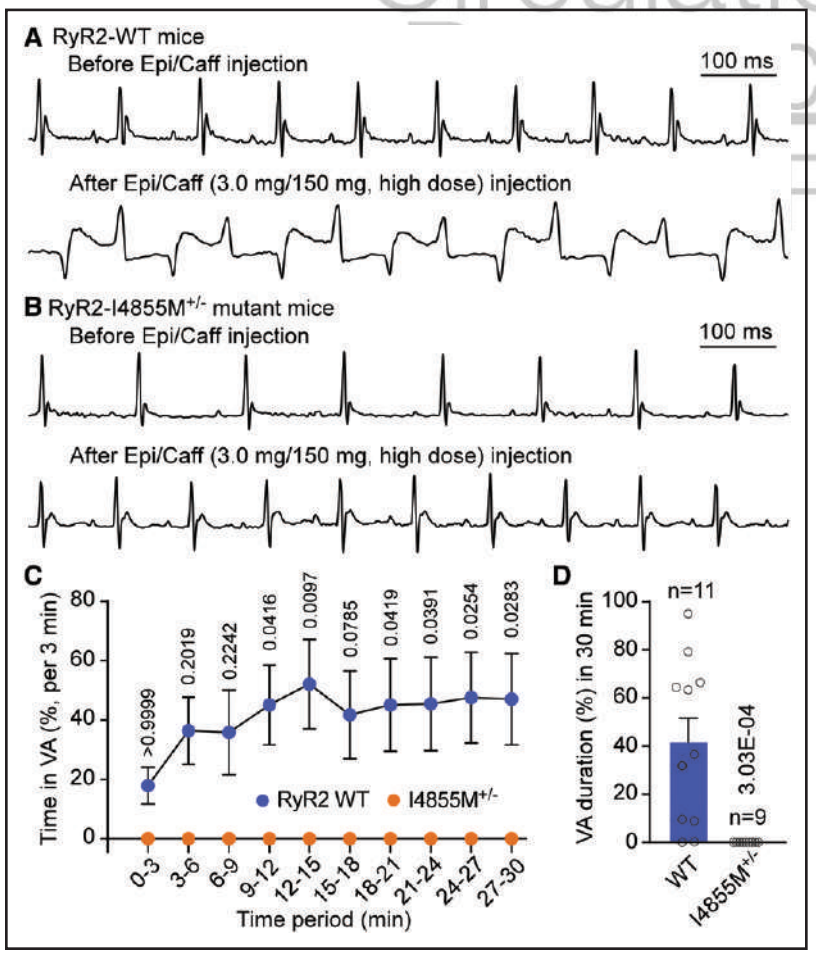

Figure 4. RyR2-I4855M mutant$^{+/-}$ mice are resilient to stress-induced catecholaminergic polymorphic ventricular tachycardia.
ECG traces of RyR2-WT (**A**) and RyR2-I4855M$^{+/-}$ mutant (**B**) mice before and after injection of epinephrine (Epi, 3.0 mg/kg) and caffeine (Caff, 150 mg/kg). Ventricular arrhythmia (VA) duration (%) within each 3 minutes (**C**) or 30 minutes (**D**) ECG recordings. Data are mean±SEM from RyR2-WT (n=11 mice) and RyR2-I4855M$^{+/-}$ mutant (n=9 mice) with the *P* values indicated for I4855M$^{+/-}$ vs WT (repeated measures ANOVA with Bonferroni's post hoc multiple comparisons test for obtaining the adjusted *P* values shown [**C**], Mann-Whitney *U* test [**D**]).

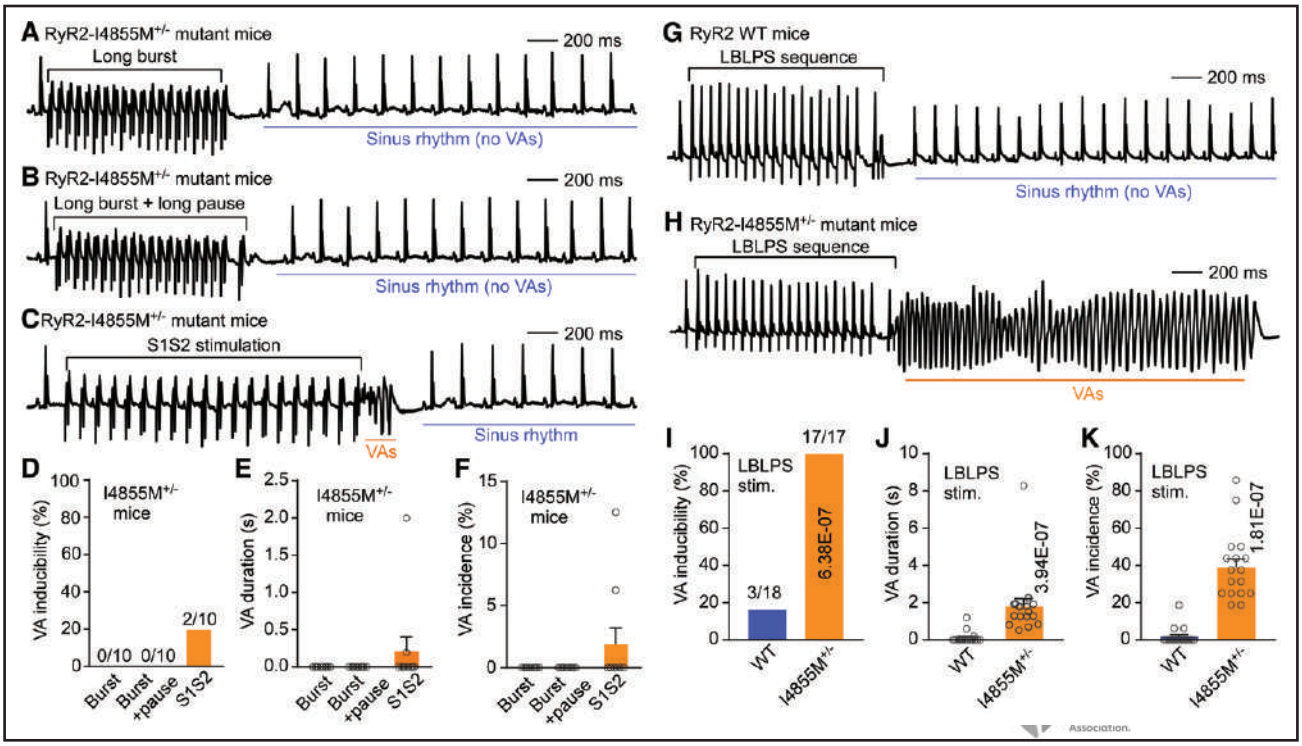

Figure 5. Ventricular arrhythmia (VA) induction in RyR2-WT and RyR2-I4855M$^{+/-}$ mutant mice by programed electrical stimulation. **A**, ECG trace after a long burst (20 beats, 60 ms interval). **B**, ECG trace after a long burst followed by a long pause (120 ms) and a stimulus. **C**, ECG trace after a basal pacing (S1, 20 beats, 100 ms interval) followed by a short-coupled extra-stimulus (S2). The S1S2 interval was progressively reduced from 78 to 18 ms with 4-ms steps. **D**, VA inducibility, (**E**) averaged VA duration, and (**F**) VA incidence in RyR2-I4855M$^{+/-}$ mutant mice paced by 3 different stimulation protocols. Data are mean±SEM from RyR2-I4855M$^{+/-}$ mutant (n=10 mice). There are no significant differences in VA inducibility (**D**) among 3 different stimulation conditions (P=0.1173, χ^2 test). There are also no significant differences in VA duration (**E**) or VA incidence (**F**) among 3 different stimulation conditions (P=0.1263, Kruskal–Wallis test with Dunn's post hoc test for both **E** and **F**). ECG traces recorded in RyR2-WT (**G**), RyR2-I4855M$^{+/-}$ mutant (**H**) mice following the long burst, long pause, and short-coupled (LBLPS) stimulation protocol. **I**, VA inducibility, (**J**) averaged VA duration, and (**K**) VA incidence in RyR2-WT and RyR2-I4855M$^{+/-}$ mutant mice after the LBLPS stimulation. Data are mean±SEM from WT (n=18 mice) and RyR2-I4855M$^{+/-}$ mutant (n=17 mice) with the P values indicated for each condition vs WT (χ^2 test [**I**] and Mann-Whitney U test [**J** and **K**]).

RyR2-I4855M$^{+/-}$ mutant mice (both males and females). Langendorff-perfused intact hearts were loaded with fluorescent Ca^{2+} dye Rhod-2 AM and electrically paced with the LBLPS stimulation protocol as described previously.[16] As shown in Figure 6, the LBLPS stimulation protocol consistently induced VA-like irregular Ca^{2+} transients in the RyR2-I4855M$^{+/-}$ mutant, but not in WT hearts (both males and females; Figure 6). Thus, isolated intact RyR2-I4855M$^{+/-}$ mutant hearts are also susceptible to LBLPS-induced VA-like irregular Ca^{2+} transients. Taken together, these observations indicate that the RyR2-I4855M$^{+/-}$ mutation can lead to CRDS as well as LVNC, and that the RyR2-I4855M$^{+/-}$ mutant mouse model recapitulates the CRDS-LVNC overlapping phenotype in humans.

The RyR2-I4855M$^{+/-}$ LOF Mutation Increases the End-Diastolic Ca^{2+} Level and the Peak Amplitude and Decay Time of Ca^{2+} Transients in Intact Hearts

It has been shown that rapid pacing induces elevation of end-diastolic Ca^{2+} level, and that such an elevation of end-diastolic Ca^{2+} level was augmented in hypertrophied hearts.[34,39,41,45] This increased end-diastolic Ca^{2+} level is thought to be one of the triggers for abnormal Ca^{2+} signaling, cardiac remodeling, and cardiomyopathies.[2,34–42,44,45] Thus, it is of interest and importance to assess whether RyR2-I4855M$^{+/-}$ mutant mice are vulnerable to rapid pacing induced elevation in end-diastolic Ca^{2+} level. To this end, we determined the end-diastolic Ca^{2+} level (delta-Fd/F0) in both male and female RyR2-WT and RyR2-I4855M$^{+/-}$ mutant hearts paced at a wide range of stimulation frequencies (3–9 Hz) using confocal intact heart Ca^{2+} imaging. We used intact hearts rather than isolated ventricular myocytes for this study, because isolated mouse ventricular myocytes hardly follow high-frequency stimulation (eg, 8–9 Hz). Consistent with those reported previously,[34,39,41,45] we found that rapid pacing induced a progressive elevation in end-diastolic Ca^{2+} level in a rate-dependent manner in both male and female RyR2-WT and RyR2-I4855M$^{+/-}$ mutant hearts (Figure 7A through 7E). Importantly, the level of end-diastolic Ca^{2+} level at each stimulation frequency (3–9 Hz) in the RyR2-I4855M$^{+/-}$ mutant hearts

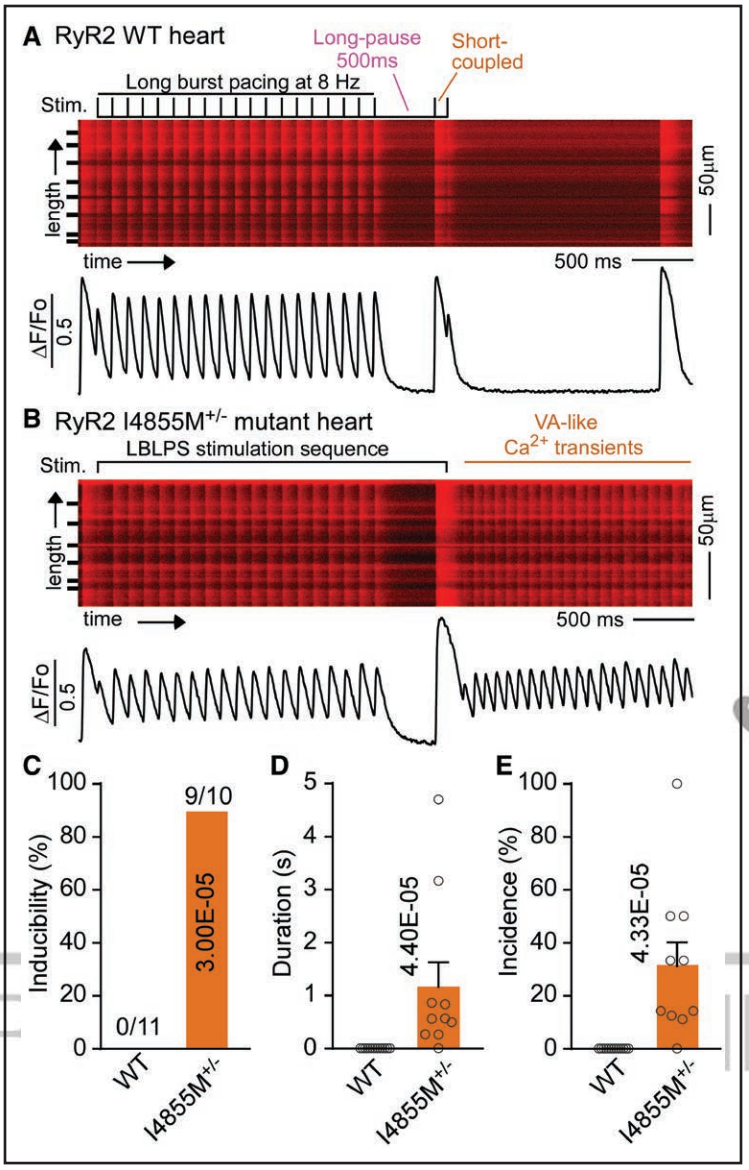

Figure 6. Long burst, long pause, and short-coupled (LBLPS) stimulation induces ventricular arrhythmia (VA)-like irregular Ca^{2+} transients in intact RyR2-I4855M$^{+/-}$ mutant hearts but not in wild-type (WT) hearts.

Intact RyR2-WT and RyR2-I4855M$^{+/-}$ mutant hearts were loaded with Rhod-2 AM. Ca^{2+} transients in intact Rhod-2 AM loaded RyR2-WT (**A**) and RyR2-I4855M$^{+/-}$ mutant (**B**) hearts during and following the LBLPS stimulation were recorded using line-scanning confocal imaging. The LBLPS protocol is depicted in **A**. Cell boundaries were indicated by short bars to the left. The ΔF/Fo traces depict the average fluorescence signal of the scan area. Scale bars: 500 ms and 50 μm, respectively. **C** Inducibility, (**D**) average duration, and (**E**) incidence of VA-like irregular Ca^{2+} transients evoked by LBLPS. Data are mean±SEM. from RyR2-WT (n=11 mice) and RyR2-I4855M$^{+/-}$ mutant (n=10 mice) with the *P* values indicated for each condition vs WT (χ^2 test [**C**] and Mann-Whitney *U* test [**D** and **E**]).

was markedly increased compared with that in the WT hearts (from both males and females; Figure 7E). Furthermore, the decay time (to 50%) and peak amplitude of depolarization-induced Ca^{2+} transients in the RyR2-I4855M$^{+/-}$ mutant hearts during rapid pacing were also markedly increased compared with those in the WT hearts (from both males and females; Figure 7F and 7G). Similarly, the peak amplitude of depolarization-induced Ca^{2+} transients in the I4855M$^{+/-}$ mutant heart after the long pause was also substantially increased compared with that in the WT hearts (from both males and females; Figure 7H). There was no significant difference in these Ca^{2+} transient properties between RyR2-I4855M$^{+/-}$ male and female hearts (Figure S6). It is of interest to note that, although both male and female RyR2-I4855M$^{+/-}$ mutant hearts exhibited increased peak amplitude and decay time of Ca^{2+} transients and elevated end-diastolic Ca^{2+} level, only males showed left ventricular hypertrophy and fibrosis (Figure 2; Figure S3). Thus, female I4855M$^{+/-}$ mutant mice appear to be protected, to some extent, against left ventricular hypertrophy and fibrosis.

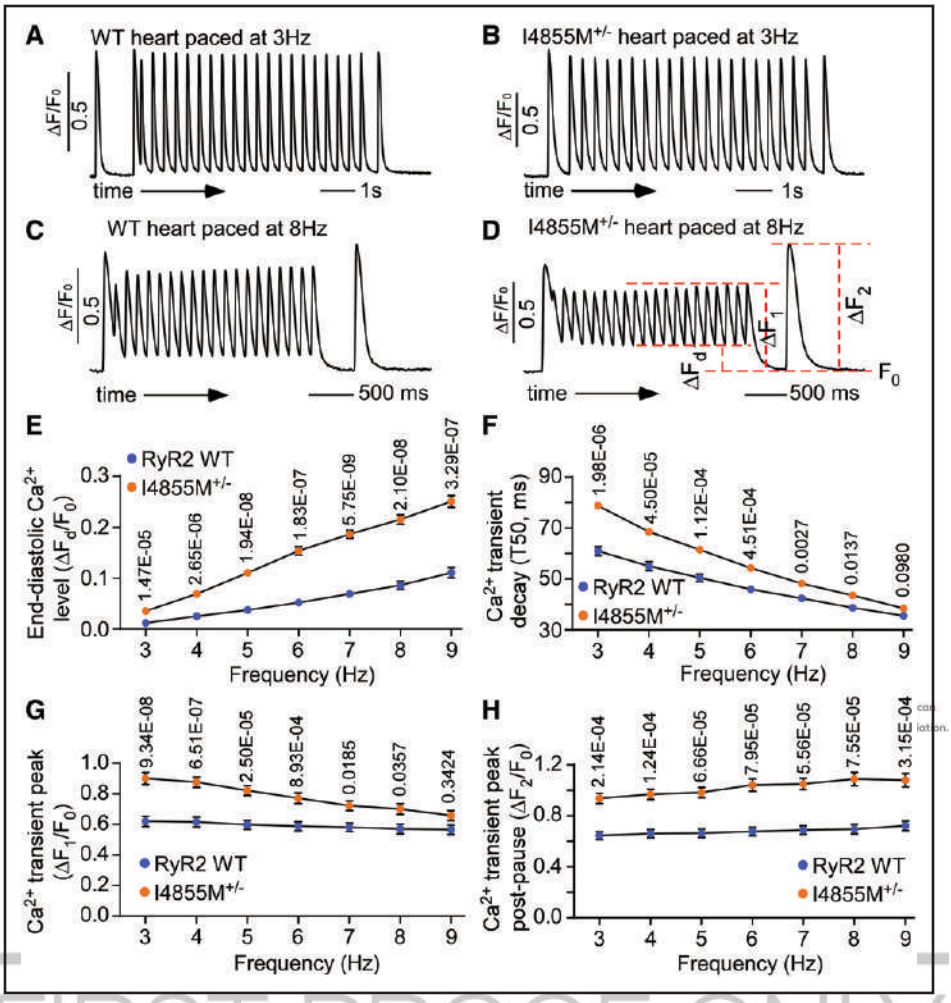

Figure 7. The RyR2-I4855M$^{+/-}$ mutation increases the end-diastolic Ca^{2+} level, the peak, and decay time of Ca^{2+} transients in intact hearts.

Ca^{2+} transients recorded in intact RyR2-wild-type (WT; **A** and **C**) and RyR2-I4855M$^{+/-}$ mutant (**B** and **D**) hearts during and following a long burst (at 3 and 8 Hz) and a long pause (500 ms) stimulation protocol (without the short-coupled extra-stimulus). **E**, End-diastolic Ca^{2+} level ($\Delta F_d/Fo$), (**F**) 50% decay time (T50) of Ca^{2+} transients, Ca^{2+} transient peak before ($\Delta F_1/Fo$; **G**) and after ($\Delta F_2/Fo$; **H**) a long pause were recorded with increased burst pacing frequencies (from 3 to 9 Hz). $\Delta F_d/Fo$, $\Delta F_1/Fo$, and $\Delta F_2/Fo$ are defined in **D**. Data are mean±SEM from RyR2-WT (n=11 mice) and RyR2-I4855M$^{+/-}$ mutant (n=10 mice) with the *P* values indicated for I4855M$^{+/-}$ vs WT (2-way ANOVA with Bonferroni post hoc test for obtaining the adjusted *P* values shown [**E–H**]).

We also performed intact heart Ca^{2+} imaging using the fluorescence Ca^{2+} dye Calbryte-520 AM that has been shown to be predominantly localized to the cytosol.[60–64] We found that the end-diastolic Ca^{2+} level, the decay time of Ca^{2+} transients, the peak amplitude of Ca^{2+} transients, and the Ca^{2+} transient peak after the pause were increased in the RyR2-I4855M$^{+/-}$ mutant hearts compared with those in WT hearts (Figure S7). We also assessed Ca^{2+} transient properties using a ratiometric fluorescence Ca^{2+} dye Cal Red-R525/650 AM. We found that the peak amplitude of Ca^{2+} transients, the end-diastolic Ca^{2+} level, and the Ca^{2+} transient decay in RyR2-I4855M$^{+/-}$ ventricular myocytes were increased compared with those in WT cells (Figure S8). These data obtained using the Calbryte-520 and Cal Red-R525/650 Ca^{2+} dyes are consistent with those observed using the Rhod-2 AM. Ca^{2+} dye. Notably, we have previously shown that the CRDS-associated RyR2-D4646A$^{+/-}$ mutant hearts without LVNC displayed an unchanged or slightly reduced peak amplitude of Ca^{2+} transients compared with RyR2 WT hearts.[16] Thus, different from the non-LVNC-associated RyR2-D4646A$^{+/-}$ mutant hearts, the LVNC-associated RyR2-I4855M$^{+/-}$ mutant hearts exhibited an increased peak amplitude of Ca^{2+} transients.

The RyR2-I4855M$^{+/-}$ LOF Mutation Elevates SR Ca^{2+} Load, Abolishes Spontaneous Ca^{2+} Release, and Increases CICR Gain

The peak amplitude of Ca^{2+} transients is, in part, determined by the SR Ca^{2+} load.[2,3,65,66] Thus, we measured

the SR Ca^{2+} content to assess whether SR Ca^{2+} content is increased in the RyR2-I4855M$^{+/-}$ LOF mutant hearts. We found that indeed the SR Ca^{2+} content in RyR2-I4855M$^{+/-}$ ventricular myocytes was markedly elevated compared with that in WT cells (from both male and female hearts; Figure 8A through 8C), which may account, in part, for the increased peak amplitude of Ca^{2+} transients (Figures 7 and 8D).

RyR2-mediated SR Ca^{2+} leak is a well-known determinant of SR Ca^{2+} load.[2,3,65,66] To assess whether the RyR2 I4855M$^{+/-}$ LOF mutation affects SR Ca^{2+} leak and thus SR Ca^{2+} load, we determined SR Ca^{2+} leak in intact RyR2 WT and I4855M$^{+/-}$ mutant hearts by measuring the propensity for store Ca^{2+} overload-induced Ca^{2+} release. We found that elevating extracellular Ca^{2+} (to produce Ca^{2+} overload) induced spontaneous SR Ca^{2+} release or leak in the form of Ca^{2+} waves in WT hearts. In contrast, there was no spontaneous Ca^{2+} release observed in RyR2-I4855M$^{+/-}$ mutant hearts (from both males and females) under the same conditions (Figure 8E through 8G). Thus, the RyR2 I4855M$^{+/-}$ LOF mutation diminishes SR Ca^{2+} leak and increases SR Ca^{2+} load, consistent with the SR Ca^{2+} leak-load relationship.[2,3,65,66]

To probe the relationship between SR Ca^{2+} load and Ca^{2+} transient decay, we plotted the decay time of systolic Ca^{2+} transients and caffeine-induced Ca^{2+} transients against the SR Ca^{2+} content (Figure S9). Consistent with the prolonged Ca^{2+} transient decay time and increased SR Ca^{2+} load observed in RyR2-I4855M$^{+/-}$ mutant cardiomyocytes (Figure 7F and 7G), these plots showed that higher SR Ca^{2+} contents were associated with longer decay times of systolic Ca^{2+} transients or caffeine-induced Ca^{2+} transients (Figure S9). This is also consistent with the previous finding that the rate of SR Ca^{2+} reuptake decreases with increasing SR Ca^{2+} content.[67]

To gain further insights into the impact of the RyR2-I4855M$^{+/-}$ mutation on SR Ca^{2+} handling, we performed immunoblotting analyses to determine the protein expression level of RyR2, SERCA2a (Sarco/endoplasmic reticulum Ca^{2+} ATPase 2a), PLB (phospholamban), and NCX (Na^+/Ca^{2+} exchanger; Figure S10), and the level of phosphorylated PLB (Figure S10) and phosphorylated RyR2 at Ser-2808 and Ser-2814 (Figure S11). We found that there was no significant difference in the expression level of RyR2, SERCA2a, total PLB (monomer or pentamer) or NCX protein (Figure S10) or the level of phosphorylated PLB-Ser-16 or phosphorylated PLB-Thr-17 (monomer or pentamer; Figure S10) or phosphorylated RyR2 at Ser-2814 (Figure S11), whereas, the phosphorylation level of RyR2 at Ser-2808 was reduced (Figure S11).

The increased peak amplitude of Ca^{2+} transients observed in the RyR2-I4855M$^{+/-}$ mutant hearts could also result from an increased L-type Ca^{2+} current. To test this possibility, we performed patch-clamp recordings

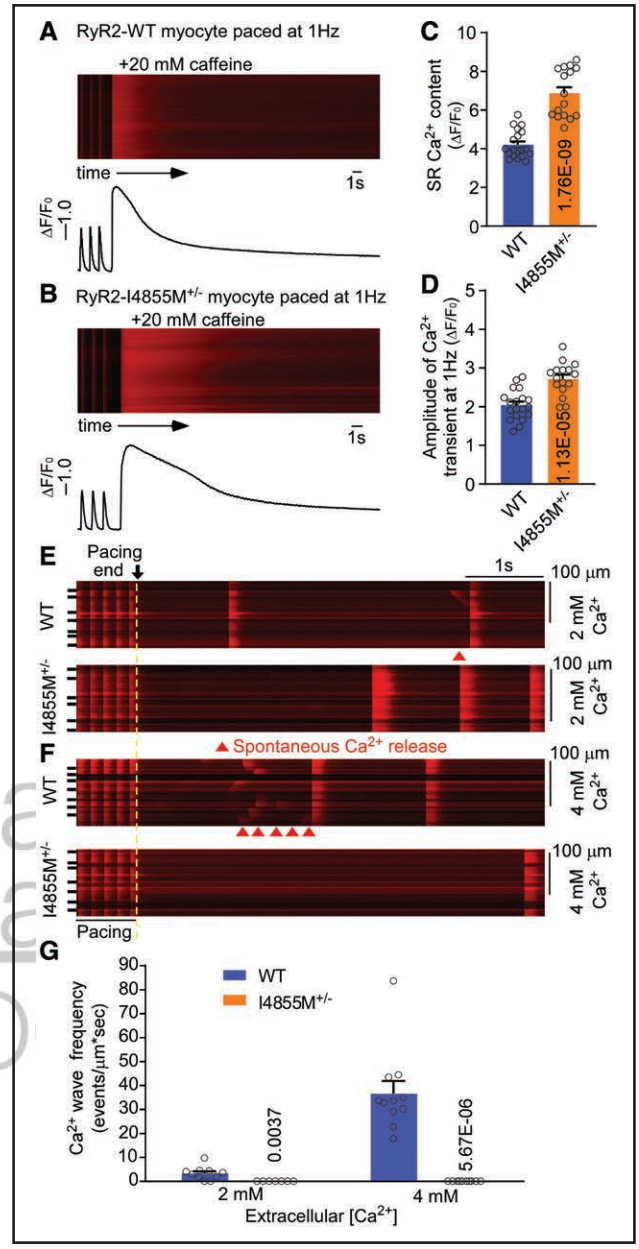

Figure 8. The I4855M loss-of-function (LOF) mutation increases sarcoplasmic reticulum (SR) Ca^{2+} content and abolishes spontaneous Ca^{2+} release.
SR Ca^{2+} contents in Rhod-2 AM loaded RyR2-WT (**A**) and RyR2-I4855M$^{+/-}$ mutant (**B**) ventricular myocytes were determined by measuring the peak of caffeine (20 mmol/L)-induced Ca^{2+} release following 1 Hz pacing. SR Ca^{2+} content (**C**), peak of Ca^{2+} transients at 1 Hz (**D**) for RyR2-WT and I4855M$^{+/-}$ mutant myocytes. Data are mean±SEM from RyR2-WT (n=19 cells, 3 hearts) and RyR2-I4855M$^{+/-}$ mutant (n=16 cells, 4 hearts) with their *P* values indicated for each condition vs control (Hierarchical statistical methods). Ca^{2+} transients in intact RyR2-WT and RyR2-I4855M$^{+/-}$ mutant hearts perfused with 2 mmol/L (**E**) or 4 mmol/L (**F**) extracellular Ca^{2+} and paced at 6 Hz followed by an abrupt cessation. Red arrowheads indicate spontaneous Ca^{2+} release events. **G**, Frequencies of spontaneous Ca^{2+} waves in WT and RyR2-I4855M$^{+/-}$ mutant hearts at 2 mmol/L or 4 mmol/L extracellular Ca^{2+}. Data are mean±SEM from RyR2-WT (n=10 mice for 2 mmol/L Ca^{2+} and 11 mice for 4 mmol/L Ca^{2+}) and RyR2-I4855M$^{+/-}$ mutant (n=7 mice for 2 mmol/L Ca^{2+} and 10 mice for 4 mmol/L Ca^{2+}) with the *P* values indicated for I4855M$^{+/-}$ vs WT (Mann-Whitney *U* test).

of the L-type Ca^{2+} current. We found that there was no significant difference in the L-type Ca^{2+} current between the RyR2-WT and RyR2-I4855M$^{+/-}$ ventricular myocytes (Figure S12). These data indicate that the increased peak amplitude of Ca^{2+} transients in RyR2-I4855M$^{+/-}$ mutant hearts did not result from an increased L-type Ca^{2+} current. Since the trigger for Ca^{2+}-induced Ca^{2+} release (CICR;, that is, the L-type Ca^{2+} current) in RyR2-WT and RyR2-I4855M$^{+/-}$ ventricular myocytes is similar, the increased peak amplitude of Ca^{2+} transients likely results from an increased CICR gain.

The RyR2-I4855M$^{+/-}$ Mutation Increases the Level of Phosphorylated CaMKII at Thr-287

To gain insights into potential mechanisms of RyR2-I4855M$^{+/-}$ mutation-associated LVNC, we performed immunoblotting analyses of some known key regulators of cardiac remodeling, including calcineurin, CaM (calmodulin), and CaMKII (Ca2+/CaM-dependent protein kinase II). We found that there was no significant difference in the protein expression level of calcineurin, CaM, or CaMKII between the RyR2-WT and RyR2-I4855M$^{+/-}$ mutant hearts (Figure S10). However, interestingly, the level of the phosphorylated CaMKII (at Thr-287) in the RyR2-I4855M$^{+/-}$ mutant hearts was significantly increased compared with WT hearts (Figure S10). This suggests that CaMKII-regulated signaling pathways[68] may be involved in RyR2-I4855M mutation-associated cardiomyopathies.

To assess the role of CaMKII in RyR2-I4855M$^{+/-}$ mutation-induced changes in Ca^{2+} transients, we performed intact heart Ca^{2+} imaging without (control) and with KN93 treatment. We found that KN-93 treatment did not significantly affect the peak amplitude of Ca^{2+} transients, peak amplitude of Ca^{2+} transients after pause, decay time of Ca^{2+} transients, or diastolic Ca^{2+} level in RyR2-I4855M$^{+/-}$ hearts (Figure S13).

DISCUSSION

Mutations in the *RYR2* gene have been linked to cardiac arrhythmias (eg, CPVT and CRDS)[4–8,16] and cardiomyopathies such as left ventricular noncompaction (LVNC).[6,17–30] The mechanisms underlying RyR2-associated cardiac arrhythmias have been extensively studied.[7,16] However, the underlying mechanism for RyR2-associated LVNC remains poorly understood. This is, in part, due to the lack of animal models for RyR2-associated LVNC. In the present study, we generated the first RyR2-associated LVNC mouse model expressing the RyR2-I4855M$^{+/-}$ LOF mutation. We showed that, as in humans, the RyR2-I4855M$^{+/-}$ LOF mutant mice displayed LVNC. In addition to LVNC, human RyR2-I4855M$^{+/-}$ mutant carriers also presented with CRDS characterized by ventricular arrhythmias and sudden death, but lack of typical CPVT phenotype.[15,16,33] Consistent with the CRDS phenotype, we also found that the RyR2-I4855M$^{+/-}$ LOF mutant mice were highly susceptible to programed electrical stimulation induced ventricular arrhythmia but are resistant to stress-induced CPVT. Thus, the RyR2-I4855M$^{+/-}$ LOF mutant mice recapitulate both the LVNC and CRDS phenotypes observed in humans and represent a novel and valuable animal model for studying the pathogenic mechanism of this CRDS-LVNC overlapping condition.

RyR2-I4855M is the first-known RyR2 LOF mutation associated with LVNC.[15,33] Previously reported LVNC-linked RyR2 mutations (RyR2-exon-3 deletion and RyR2-R169Q) are GOF. The mechanisms by which both LOF and GOF RyR2 mutations cause LVNC are currently unknown. An unexpected finding of the present study is that the RyR2-I4855M$^{+/-}$ LOF mutation increased the peak amplitude of depolarization-induced Ca^{2+} transients in cardiomyocytes. We have previously shown that the RyR2-I4855M$^{+/-}$ mutation abolished store overload induced spontaneous Ca^{2+} release in HEK293 cells.[16] We have now shown that the RyR2-I4855M$^{+/-}$ mutation also diminished spontaneous SR Ca^{2+} release or leak in cardiomyocytes in intact working hearts. These observations suggest that the RyR2-I4855M$^{+/-}$ mutation exerts an effect on spontaneous SR Ca^{2+} release different from that on depolarization-induced Ca^{2+} release (ie, it diminishes the former but increases the latter). How the RyR2-I4855M$^{+/-}$ LOF mutation could lead to seemingly paradoxical impact on RyR2 function is unclear. SR Ca^{2+} leak has a major impact on SR Ca^{2+} load.[2,3,65,66,69] Thus, diminished SR Ca^{2+} leak is expected to increase SR Ca^{2+} load. Indeed, we found that the SR Ca^{2+} content in RyR2-I4855M$^{+/-}$ LOF mutant cardiomyocytes was markedly elevated compared with that in WT cells. The increased SR Ca^{2+} load is unlikely to be due to changes in the level of RyR2, phosphorylated RyR2-S2814, SERCA2a, PLB, phosphorylated PLB or NCX, all of which were not significantly different between RyR2-WT and RyR2-I4855M$^{+/-}$ mutant hearts. The diminished SR Ca^{2+} leak and the resulting increased SR Ca^{2+} load observed in the RyR2-I4855M$^{+/-}$ mutant hearts is likely to result from the impact of the I4855M mutation on the intrinsic properties of the RyR2 channel. Furthermore, given the well-established relationship between SR Ca^{2+} load and SR Ca^{2+} release,[2,3,65,66,69] elevated SR Ca^{2+} load is expected to increase the peak amplitude of SR Ca^{2+} release. Consistent with this, we found that the peak amplitude of Ca^{2+} transients in RyR2-I4855M$^{+/-}$ LOF mutant hearts was substantially increased compared with that in WT hearts. The peak amplitude of Ca^{2+} transients could also be influenced by the L-type Ca^{2+} current (the trigger for Ca^{2+} induced Ca^{2+} release, CICR) and the CICR gain. Our patch-clamp recordings revealed that there was no significant difference in the L-type Ca^{2+} current between the RyR2-WT and RyR2-I4855M$^{+/-}$ mutant ventricular

myocytes. Thus, the unchanged L-type Ca^{2+} current and increased peak amplitude of Ca^{2+} transients suggest that the CICR gain in RyR2-I4855M$^{+/-}$ mutant ventricular myocytes is increased compared with that in WT cells. Taken together, the RyR2-I4855M$^{+/-}$ LOF mutation may increase the peak amplitude of Ca^{2+} transients by increasing the CICR gain as a result of diminished SR Ca^{2+} leak and elevated SR Ca^{2+} load.

We have previously shown that the CRDS-associated RyR2-D4646A$^{+/-}$ LOF mutant mouse model displayed no marked differences in cardiac structure/morphology compared with WT mice.[16] Furthermore, we found that there was no significant difference in the ratio of the non—compaction (NC) ventricular layer over the compacted (C) ventricular layer (ie, the NC/C ratio) between RyR2-WT and RyR2-D4646A$^{+/-}$ mutant hearts. Thus, as in human patients harboring the RyR2-D4646A$^{+/-}$ mutation, the CRDS RyR2-D4646A$^{+/-}$ mouse model does not display LVNC. Importantly, different from the RyR2-I4855M$^{+/-}$ mutant hearts, the RyR2-D4646A$^{+/-}$ mutant hearts displayed an unchanged or slightly reduced peak amplitude of Ca^{2+} transients and a markedly increased L-type Ca^{2+} current compared with the RyR2-WT hearts.[16] The unchanged peak amplitude of Ca^{2+} transients and the increased L-type Ca^{2+} current would suggest that the CICR gain in RyR2-D4646A$^{+/-}$ mutant ventricular myocytes is reduced compared with that in WT cells. This is opposite to the increased CICR gain in RyR2-I4855M$^{+/-}$ cells. Together, these comparisons between LVNC-associated RyR2-I4855M$^{+/-}$ and non-LVNC-associated RyR2-D4646A$^{+/-}$ mutant hearts suggest that an increased peak amplitude of Ca^{2+} transients may represent an important determinant of RyR2-associated LVNC.

It is well known that elevated SR Ca^{2+} load not only can enhance the amplitude of Ca^{2+} transients, but also can increase the decay time of Ca^{2+} transients.[2,3,65–67] Consistent with this view, we found that the RyR2-I4855M$^{+/-}$ mutation not only elevated SR Ca^{2+} load, but also prolonged Ca^{2+} transient decay. However, given that the RyR2-I4855M$^{+/-}$ mutant hearts displayed substantial structural and functional remodeling, it is unlikely that the prolonged decay time of Ca^{2+} transients observed in the RyR2-I4855M$^{+/-}$ mutant heart is only due to increased SR Ca^{2+} load. It is more likely that there are other RyR2-I4855M mutation-induced changes that may also affect the decay time of Ca^{2+} transients.

Furthermore, the level of end-diastolic Ca^{2+} level during rapid pacing is dependent on the rate of Ca^{2+} transient decay. A prolonged Ca^{2+} transient decay would be expected to increase end-diastolic Ca^{2+} level during rapid pacing. Indeed, we found that the RyR2-I4855M$^{+/-}$ mutant hearts exhibited an increased end-diastolic Ca^{2+} level during rapid pacing compared with WT hearts. Thus, the elevated SR Ca^{2+} load as a result of diminished SR Ca^{2+} leak likely contributes, in part, to the prolonged Ca^{2+} transient decay and increased end-diastolic Ca^{2+} level during rapid pacing in the RyR2-I4855M$^{+/-}$ mutant hearts.

It is well established that the end-diastolic Ca^{2+} level is a critical determinant of Ca^{2+}-dependent cardiac remodeling and cardiomyopathies.[2,34–45] It has been shown that hypertrophied hearts displayed increased end-diastolic Ca^{2+} level, especially at rapid heart rates compared with WT hearts.[34,41,45] Thus, this increased end-diastolic Ca^{2+} level together with the increased peak amplitude of Ca^{2+} transients may initiate the Ca^{2+} signaling cascade that can lead to cardiac remodeling and hypertrophic signaling.[2,35–40,42–44] Consistent with this view, we found that the level of the phosphorylated CaMKII (at Thr-287) in RyR2-I4855M$^{+/-}$ mutant hearts was significantly increased compared with WT hearts, whereas there was no significant difference in the protein expression level of calcineurin, CaM, or total CaMKII between the RyR2-WT and RyR2-I4855M$^{+/-}$ mutant hearts. This suggests that CaMKII-regulated signaling pathways[68] may be involved in RyR2-I4855M$^{+/-}$ mutation-associated cardiomyopathy. However, treatment with KN93 did not significantly affect the peak amplitude of Ca^{2+} transients, decay time of Ca^{2+} transients, or diastolic Ca^{2+} level in RyR2-I4855M$^{+/-}$ hearts. These data suggest that, although CaMKII-regulated signaling pathways may be involved in the development of RyR2-I4855M mutation-associated LVNC, CaMKII may not play a critical role in the RyR2-I4855M$^{+/-}$ mutation-induced alterations in Ca^{2+} transient properties. The altered Ca^{2+} transient properties observed in the RyR2-I4855M$^{+/-}$ mutant hearts may result primarily from the impact of the I4855M$^{+/-}$ mutation on the intrinsic gating properties of the RyR2 channel.

Our present study revealed that both female and male RyR2-I4855M$^{+/-}$ mutant mice displayed LVNC; however, only male RyR2 I4855M$^{+/-}$ mutant mice exhibited a significantly increased heart/body weight ratio, cell size, and left ventricular fibrosis compared with RyR2-WT mice. Furthermore, we showed that male but not female RyR2-I4855M$^{+/-}$ mutant mice exhibited left ventricular hypertrophic phenotype. On the other hand, both male and female RyR2-I4855M$^{+/-}$ mutant mice showed reduced heart rate, increased isovolumic relaxation time, increased left ventricular mass, and left atrium hypertrophy. Thus, female RyR2-I4855M$^{+/-}$ mutant mice are unlikely to be completely protected against cardiac hypertrophy.

Study Limitations

As with female RyR2-I4855M$^{+/-}$ mutant mice, human female RyR2-I4855M$^{+/-}$ mutant carriers presented with LVNC but no left ventricular hypertrophy. The mechanism underlying this sex-dependent difference has yet to be defined. Interestingly, in the family harboring the RyR2-I4855M$^{+/-}$ mutation, all mutant carriers were females, and there were no affected males. Hence, whether the I4855M$^{+/-}$ mutation can cause LVNC and left ventricular

hypertrophy and fibrosis in human male mutant carriers has yet to be determined. Furthermore, it is unclear whether hypertrophic phenotype would occur in female RyR2-I4855M$^{+/-}$ mutant mice at older ages. The age-dependence of the hypertrophic phenotype in the RyR2-I4855M$^{+/-}$ mutant mice is an important issue and further detailed and systematic studies would be required. Moreover, given the cytosolic and mitochondrial localization of the Rhod-2 AM fluorescence Ca^{2+} dye, our Rhod-2 AM-based intracellular Ca^{2+} measurements would reflect Ca^{2+} levels in both the cytosol and mitochondria. To monitor cytosolic Ca^{2+} dynamics more specifically and accurately, we employed the fluorescence Ca^{2+} dye Calbryte 520-AM that has been shown to be predominantly localized in the cytosol and the ratiometric fluorescence Ca^{2+} dye Cal Red-R525/650 AM. Importantly, consistent with those observed using the Rhod-2 AM. Ca^{2+} dye, Ca^{2+} imaging experiments using the Calbryte 520 AM and Cal Red-R525/650 Ca^{2+} dyes also revealed that the peak amplitude of Ca^{2+} transients, the end-diastolic Ca^{2+} level, and the Ca^{2+} transient decay in RyR2-I4855M$^{+/-}$ ventricular myocytes were increased compared with those in WT cells. It should also be noted that to avoid motion artifact, we inhibited muscle contraction in our ex vivo intact working heart Ca^{2+} imaging using blebbistatin, which may influence Ca^{2+} measurements.

In summary, we generated the first RyR2-associated LVNC mouse model that recapitulates the CRDS and LVNC overlapping phenotype in humans. Unexpectedly, the CRDS-LVNC-associated RyR2-I4855M$^{+/-}$ LOF mutation increased the peak amplitude of Ca^{2+} transients and end-diastolic Ca^{2+} level, which are well-known Ca^{2+} handling abnormalities that can lead to cardiac remodeling and hypertrophic signaling. Thus, targeting the peak-systolic and end-diastolic Ca^{2+} levels may offer a therapeutic strategy for RyR2-associated LVNC.

ARTICLE INFORMATION

Received January 4, 2023; revision received May 30, 2023; accepted June 7, 2023.

Affiliations

Department of Physiology and Pharmacology, Libin Cardiovascular Institute, University of Calgary, Alberta, Canada (M.N., Y.L., J.W., Z.S., H.W., J.Y., Y.-X.C., D.B., J.P.E., R.W., S.R.W.C.). School of Medicine, Northwest University, Xi 'an, China (J.W.). Department of Automatic Control, Universitat Politècnica de Catalunya, Barcelona, Spain (A.V., R.B.). Institut de Recerca Sant Joan de Déu (IRSJD), Barcelona, Spain (R.B.). Biomedical Research Institute Barcelona IIBB-CSIC, IIB Sant Pau and CIBERCV, Hospital de Sant Pau, Barcelona, Spain (L.H.-M.). Department of Medicine, School of Medicine, University of California, San Diego, La Jolla (W.F., J.C.). Division of Pediatric Cardiology, Department of Pediatrics (T.M.R., S.S.) and Department of Medical Genetics (A.L.), University of British Columbia, Vancouver, Canada.

Acknowledgments

M. Ni, Y. Li, J. Wei, Z. Song, J. Yao, Y-X. Chen, D. Belke, R. Wang, A, Vallmitjana, R. Benitez, L. Hove-Madsen, J. Chen, T.M. Roston, S. Sanatani, A. Lehman, and S.R.W. Chen designed the research. M. Ni, Y. Li, J. Wei, Z. Song, H. Wang, J. Yao, Y-X. Chen, D. Belke, J.P. Estillore, R. Wang, A, Vallmitjana, R. Benitez, and W. Feng performed the research. M. Ni, Y. Li, J. Wei, Z. Song, H. Wang, J. Yao, Y-X. Chen, D. Belke, A, Vallmitjana, R. Benitez, L. Hove-Madsen, and S.R.W. Chen analyzed data. M. Ni, R. Wang, L. Hove-Madsen, and S.R.W. Chen wrote the article.

Sources of Funding

This work was supported by research grants from the Canadian Rare Diseases: Models and Mechanisms Network (RDMM; 150129-001-001) to S.R. Wayne Chen and A. Lehman, the Canadian Institutes of Health Research (PJT-155940) to S.R. Wayne Chen, the Spanish Ministry of Science Innovation and Universities PID2020-116927RB-C21 and -C22 (to L. Hove-Madsen and R. Benitez), Marato-TV3 20152030 (to L. Hove-Madsen) and Generalitat de Catalunya SGR2017-1769 (to L. Hove-Madsen). S.R. Wayne Chen holds the Heart and Stroke Foundation Chair in Cardiovascular Research (END611955).

Disclosures

J. Wei and H. Wang, recipients of the Libin Cardiovascular Institute of Alberta and Cumming School of Medicine Postdoctoral Fellowship Award. Z. Song, recipient of the University of Calgary Eyes High Postdoctoral Fellowship Award. J. Yao, recipient of the Alberta Innovates-Health Solutions (AIHS) Fellowship Award. T.M. Roston, supported by the University of British Columbia Clinician Investigator Program, and a UBC Friedman Scholar in Health and CHRS George Mines Travelling Fellow in Cardiac Electrophysiology. S.R.W. Chen, Heart and Stroke Foundation Chair in Cardiovascular Research. The other authors report no conflicts.

Supplemental Material

Expanded Materials and Methods
Figures S1–S13
References 70–76

REFERENCES

1. Bers DM. Cardiac excitation-contraction coupling. *Nature*. 2002;415:198–205. doi: 10.1038/415198a
2. Bers DM. Calcium cycling and signaling in cardiac myocytes. *Annu Rev Physiol*. 2008;70:23–49. doi: 10.1146/annurev.physiol.70.113006.100455
3. Bers DM. Cardiac sarcoplasmic reticulum calcium leak: basis and roles in cardiac dysfunction. *Annu Rev Physiol*. 2014;76:107–127. doi: 10.1146/annurev-physiol-020911-153308
4. Priori SG, Napolitano C, Tiso N, Memmi M, Vignati G, Bloise R, Sorrentino VV, Danieli GA. Mutations in the cardiac ryanodine receptor gene (hRyR2) underlie catecholaminergic polymorphic ventricular tachycardia. *Circulation*. 2001;103:196–200. doi: 10.1161/01.cir.103.2.196
5. Napolitano C, Priori SG. Diagnosis and treatment of catecholaminergic polymorphic ventricular tachycardia. *Heart Rhythm*. 2007;4:675–678. doi: 10.1016/j.hrthm.2006.12.048
6. Medeiros-Domingo A, Bhuiyan ZA, Tester DJ, Hofman N, Bikker H, van Tintelen JP, Mannens MM, Wilde AA, Ackerman MJ. The RYR2-encoded ryanodine receptor/calcium release channel in patients diagnosed previously with either catecholaminergic polymorphic ventricular tachycardia or genotype negative, exercise-induced long QT syndrome: a comprehensive open reading frame mutational analysis. *J Am Coll Cardiol*. 2009;54:2065–2074. doi: 10.1016/j.jacc.2009.08.022
7. Priori SG, Chen SR. Inherited dysfunction of sarcoplasmic reticulum Ca^{2+} handling and arrhythmogenesis. *Circ Res*. 2011;108:871–883. doi: 10.1161/CIRCRESAHA.110.226845
8. Lieve KV, van der Werf C, Wilde AA. Catecholaminergic polymorphic ventricular tachycardia. *Circ J*. 2016;80:1285–1291. doi: 10.1253/circj.CJ-16-0326
9. Wleklinski MJ, Kannankeril PJ, Knollmann BC. Molecular and tissue mechanisms of catecholaminergic polymorphic ventricular tachycardia. *J Physiol*. 2020;598:2817–2834. doi: 10.1113/JP276757
10. Priori SG, Napolitano C, Memmi M, Colombi B, Drago F, Gasparini M, DeSimone L, Coltorti F, Bloise R, Keegan R, et al. Clinical and molecular characterization of patients with catecholaminergic polymorphic ventricular tachycardia. *Circulation*. 2002;106:69–74. doi: 10.1161/01.cir.0000020013.73106.d8
11. Jiang D, Chen W, Wang R, Zhang L, Chen SRW. Loss of luminal Ca^{2+} activation in the cardiac ryanodine receptor is associated with ventricular fibrillation and sudden death. *Proc Natl Acad Sci USA*. 2007;104:18309–18314. doi: 10.1073/pnas.0706573104
12. Paech C, Gebauer RA, Karstedt J, Marschall C, Bollmann A, Husser D. Ryanodine receptor mutations presenting as idiopathic ventricular fibrillation: a report on two novel familial compound mutations, c.6224T>C and c.13781A>G, with the clinical presentation of idiopathic ventricular fibrillation. *Pediatr Cardiol*. 2014;35:1437–1441. doi: 10.1007/s00246-014-0950-2
13. Zhao YT, Valdivia CR, Gurrola GB, Powers PP, Willis BC, Moss RL, Jalife J, Valdivia HH. Arrhythmogenesis in a catecholaminergic polymorphic ventricular tachycardia mutation that depresses ryanodine receptor function. *Proc Natl Acad Sci USA*. 2015;112:E1669–E1677. doi: 10.1073/pnas.1419795112

14. Fujii Y, Itoh H, Ohno S, Murayama T, Kurebayashi N, Aoki H, Blancard M, Nakagawa Y, Yamamoto S, Matsui Y, et al. A type 2 ryanodine receptor variant associated with reduced Ca^{2+} release and short-coupled torsades de pointes ventricular arrhythmia. *Heart Rhythm*. 2017;14:98–107. doi: 10.1016/j.hrthm.2016.10.015
15. Roston TM, Guo W, Krahn AD, Wang R, Van Petegem F, Sanatani S, Chen SR, Lehman A. A novel RYR2 loss-of-function mutation (I4855M) is associated with left ventricular non-compaction and atypical catecholaminergic polymorphic ventricular tachycardia. *J Electrocardiol*. 2017;50:227–233. doi: 10.1016/j.jelectrocard.2016.09.006
16. Sun B, Yao J, Ni M, Wei J, Zhong X, Guo W, Zhang L, Wang R, Belke D, Chen YX, et al. Cardiac ryanodine receptor calcium release deficiency syndrome. *Sci Transl Med*. 2021;13:eaba7287. doi: 10.1126/scitranslmed.aba7287
17. Tiso N, Stephan DA, Nava A, Bagattin A, Devaney JM, Stanchi F, Larderet G, Brahmbhatt B, Brown K, Bauce B, et al. Identification of mutations in the cardiac ryanodine receptor gene in families affected with arrhythmogenic right ventricular cardiomyopathy type 2 (ARVD2). *Hum Mol Genet*. 2001;10:189–194. doi: 10.1093/hmg/10.3.189
18. Bauce B, Rampazzo A, Basso C, Bagattin A, Daliento L, Tiso N, Turrini P, Thiene G, Danieli GA, Nava A. Screening for ryanodine receptor type 2 mutations in families with effort-induced polymorphic ventricular arrhythmias and sudden death: early diagnosis of asymptomatic carriers. *J Am Coll Cardiol*. 2002;40:341–349. doi: 10.1016/s0735-1097(02)01946-0
19. Tester DJ, Spoon DB, Valdivia HH, Makielski JC, Ackerman MJ. Targeted mutational analysis of the RyR2-encoded cardiac ryanodine receptor in sudden unexplained death: a molecular autopsy of 49 medical examiner/coroner's cases. *Mayo Clin Proc*. 2004;79:1380–1384. doi: 10.4065/79.11.1380
20. d'Amati G, Bagattin A, Bauce B, Rampazzo A, Autore C, Basso C, King K, Romeo MD, Gallo P, Thiene G, et al. Juvenile sudden death in a family with polymorphic ventricular arrhythmias caused by a novel RyR2 gene mutation: evidence of specific morphological substrates. *Hum Pathol*. 2005;36:761–767. doi: 10.1016/j.humpath.2005.04.019
21. Nishio H, Iwata M, Suzuki K. Postmortem molecular screening for cardiac ryanodine receptor type 2 mutations in sudden unexplained death: R420W mutated case with characteristics of status thymico-lymphatics. *Circ J*. 2006;70:1402–1406. doi: 10.1253/circj.70.1402
22. Noboru F, Hidekazu I, Kenshi H, Katsuharu U, Mitsuru N, Tetsuo K, Hiromasa K, Yuichiro S, Toshinari T, Kazuo O, et al. A novel missense mutation in cardiac ryanodine receptor gene as a possible cause of hypertrophic cardiomyopathy: evidence from familial analysis. *Circulation*. 2006;114:165.
23. Alvarado FJ, Bos JM, Yuchi Z, Valdivia CR, Hernández JJ, Zhao YT, Henderlong DS, Chen Y, Booher TR, Marcou CA, et al. Cardiac hypertrophy and arrhythmia in mice induced by a mutation in ryanodine receptor 2. *JCI insight*. 2019;5:e126544. doi: 10.1172/jci.insight.126544
24. Bhuiyan ZA, van den Berg MP, van Tintelen JP, Bink-Boelkens MT, Wiesfeld AC, Alders M, Postma AV, van Langen I, Mannens MM, Wilde AA. Expanding spectrum of human RYR2-related disease: new electrocardiographic, structural, and genetic features. *Circulation*. 2007;116:1569–1576. doi: 10.1161/CIRCULATIONAHA.107.711606
25. Marjamaa A, Laitinen-Forsblom P, Lahtinen AM, Viitasalo M, Toivonen L, Kontula K, Swan H. Search for cardiac calcium cycling gene mutations in familial ventricular arrhythmias resembling catecholaminergic polymorphic ventricular tachycardia. *BMC Med Genet*. 2009;10:12. doi: 10.1186/1471-2350-10-12
26. Szentpáli Z, Szili-Torok T, Caliskan K. Primary electrical disorder or primary cardiomyopathy? A case with a unique association of noncompaction cardiomyopathy and cathecolaminergic polymorphic ventricular tachycardia caused by ryanodine receptor mutation. *Circulation*. 2013;127:1165–1166. doi: 10.1161/CIRCULATIONAHA.112.144949
27. Ohno S, Omura M, Kawamura M, Kimura H, Itoh H, Makiyama T, Ushinohama H, Makita N, Horie M. Exon 3 deletion of RYR2 encoding cardiac ryanodine receptor is associated with left ventricular non-compaction. *Europace*. 2014;16:1646–1654. doi: 10.1093/europace/eut382
28. Campbell MJ, Czosek RJ, Hinton RB, Miller EM. Exon 3 deletion of ryanodine receptor causes left ventricular noncompaction, worsening catecholaminergic polymorphic ventricular tachycardia, and sudden cardiac arrest. *Am J Med Genet A*. 2015;167a:2197–2200. doi: 10.1002/ajmg.a.37140
29. Dharmawan T, Nakajima T, Ohno S, Iizuka T, Tamura S, Kaneko Y, Horie M, Kurabayashi M. Identification of a novel exon3 deletion of RYR2 in a family with catecholaminergic polymorphic ventricular tachycardia. *Ann Noninvasive Electrocardiol*. 2019;24:e12623. doi: 10.1111/anec.12623
30. Kohli U, Aziz Z, Beaser AD, Nayak HM. A large deletion in RYR2 exon 3 is associated with nadolol and flecainide refractory catecholaminergic polymorphic ventricular tachycardia. *Pacing Clin Electrophysiol*. 2019;42:1146–1154. doi: 10.1111/pace.13668
31. Tang Y, Tian X, Wang R, Fill M, Chen SR. Abnormal termination of Ca^{2+} release is a common defect of RyR2 mutations associated with cardiomyopathies. *Circ Res*. 2012;110:968–977. doi: 10.1161/CIRCRESAHA.111.256560
32. Nozaki Y, Kato Y, Uike K, Yamamura K, Kikuchi M, Yasuda M, Ohno S, Horie M, Murayama T, Kurebayashi N, et al. Co-phenotype of left ventricular non-compaction cardiomyopathy and atypical catecholaminergic polymorphic ventricular tachycardia in association with R169Q, a ryanodine receptor type 2 missense mutation. *Circ J*. 2020;84:226–234. doi: 10.1253/circj.CJ-19-0720
33. Roston TM, Sanatani S, Chen SR. Suppression-of-function mutations in the cardiac ryanodine receptor: emerging evidence for a novel arrhythmia syndrome? *Heart Rhythm*. 2017;14:108–109. doi: 10.1016/j.hrthm.2016.11.004
34. Gwathmey JK, Warren SE, Briggs GM, Copelas L, Feldman MD, Phillips PJ, Callahan M Jr, Schoen FJ, Grossman W, Morgan JP. Diastolic dysfunction in hypertrophic cardiomyopathy. Effect on active force generation during systole. *J Clin Invest*. 1991;87:1023–1031. doi: 10.1172/JCI115061
35. Molkentin JD, Lu JR, Antos CL, Markham B, Richardson J, Robbins J, Grant SR, Olson EN. A calcineurin-dependent transcriptional pathway for cardiac hypertrophy. *Cell*. 1998;93:215–228. doi: 10.1016/s0092-8674(00)81573-1
36. Passier R, Zeng H, Frey N, Naya FJ, Nicol RL, McKinsey TA, Overbeek P, Richardson JA, Grant SR, Olson EN. CaM kinase signaling induces cardiac hypertrophy and activates the MEF2 transcription factor in vivo. *J Clin Invest*. 2000;105:1395–1406. doi: 10.1172/JCI8551
37. Fatkin D, McConnell BK, Mudd JO, Semsarian C, Moskowitz IG, Schoen FJ, Giewat M, Seidman CE, Seidman JG. An abnormal Ca^{2+} response in mutant sarcomere protein-mediated familial hypertrophic cardiomyopathy. *J Clin Invest*. 2000;106:1351–1359. doi: 10.1172/JCI11093
38. Wilkins BJ, Molkentin JD. Calcineurin and cardiac hypertrophy: where have we been? Where are we going? *J Physiol*. 2002;541:1–8. doi: 10.1113/jphysiol.2002.017129
39. Robinson P, Griffiths PJ, Watkins H, Redwood CS. Dilated and hypertrophic cardiomyopathy mutations in troponin and alpha-tropomyosin have opposing effects on the calcium affinity of cardiac thin filaments. *Circ Res*. 2007;101:1266–1273. doi: 10.1161/CIRCRESAHA.107.156380
40. Houser SR, Molkentin JD. Does contractile Ca^{2+} control calcineurin-NFAT signaling and pathological hypertrophy in cardiac myocytes? *Sci Signaling*. 2008;1:pe31. doi: 10.1126/scisignal.125pe31
41. Schober T, Huke S, Venkataraman R, Gryshchenko O, Kryshtal D, Hwang HS, Baudenbacher FJ, Knollmann BC. Myofilament Ca sensitization increases cytosolic Ca binding affinity, alters intracellular Ca homeostasis, and causes pause-dependent Ca-triggered arrhythmia. *Circ Res*. 2012;111:170–179. doi: 10.1161/CIRCRESAHA.112.270041
42. Coppini R, Ferrantini C, Yao L, Fan P, Del Lungo M, Stillitano F, Sartiani L, Tosi B, Suffredini S, Tesi C, et al. Late sodium current inhibition reverses electromechanical dysfunction in human hypertrophic cardiomyopathy. *Circulation*. 2013;127:575–584. doi: 10.1161/CIRCULATIONAHA.112.134932
43. Lan F, Lee AS, Liang P, Sanchez-Freire V, Nguyen PK, Wang L, Han L, Yen M, Wang Y, Sun N, et al. Abnormal calcium handling properties underlie familial hypertrophic cardiomyopathy pathology in patient-specific induced pluripotent stem cells. *Cell stem cell*. 2013;12:101–113. doi: 10.1016/j.stem.2012.10.010
44. Coppini R, Mazzoni L, Ferrantini C, Gentile F, Pioner JM, Laurino A, Santini L, Bargelli V, Rotellini M, Bartolucci G, et al. Ranolazine prevents phenotype development in a mouse model of hypertrophic cardiomyopathy. *Circ Heart Fail*. 2017;10:e003565. doi: 10.1161/CIRCHEARTFAILURE.116.003565
45. Robinson P, Liu X, Sparrow A, Patel S, Zhang YH, Casadei B, Watkins H, Redwood C. Hypertrophic cardiomyopathy mutations increase myofilament Ca^{2+} buffering, alter intracellular Ca^{2+} handling, and stimulate Ca^{2+}-dependent signaling. *J Biol Chem*. 2018;293:10487–10499. doi: 10.1074/jbc.RA118.002081
46. Ikeda U, Minamisawa M, Koyama J. Isolated left ventricular noncompaction cardiomyopathy in adults. *J Cardiol*. 2015;65:91–97. doi: 10.1016/j.jjcc.2014.10.005
47. Stöllberger C, Finsterer J. Left ventricular hypertrabeculation/noncompaction. *J Am Soc Echocardiogr*. 2004;17:91–100. doi: 10.1016/s0894-7317(03)00514-5
48. Finsterer J, Stöllberger C, Bonner E. Acquired noncompaction associated with coronary heart disease and myopathy. *Heart Lung*. 2010;39:240–241. doi: 10.1016/j.hrtlng.2009.09.001
49. Oechslin E, Jenni R. Left ventricular non-compaction revisited: a distinct phenotype with genetic heterogeneity? *Eur Heart J*. 2011;32:1446–1456. doi: 10.1093/eurheartj/ehq508
50. Hussein A, Karimianpour A, Collier P, Krasuski RA. Isolated noncompaction of the left ventricle in adults. *J Am Coll Cardiol*. 2015;66:578–585. doi: 10.1016/j.jacc.2015.06.017

51. Arbustini E, Favalli V, Narula N, Serio A, Grasso M. Left ventricular noncompaction: a distinct genetic cardiomyopathy? *J Am Coll Cardiol*. 2016;68:949–966. doi: 10.1016/j.jacc.2016.05.096
52. Takasaki A, Hirono K, Hata Y, Wang C, Takeda M, Yamashita JK, Chang B, Nakaoka H, Okabe M, Miyao N, et al. Sarcomere gene variants act as a genetic trigger underlying the development of left ventricular noncompaction. *Pediatr Res*. 2018;84:733–742. doi: 10.1038/s41390-018-0162-1
53. Weber KT, Janicki JS, Shroff SG, Pick R, Chen RM, Bashey RI. Collagen remodeling of the pressure-overloaded, hypertrophied nonhuman primate myocardium. *Circ Res*. 1988;62:757–765. doi: 10.1161/01.res.62.4.757
54. Factor SM, Butany J, Sole MJ, Wigle ED, Williams WC, Rojkind M. Pathologic fibrosis and matrix connective tissue in the subaortic myocardium of patients with hypertrophic cardiomyopathy. *J Am Coll Cardiol*. 1991;17:1343–1351. doi: 10.1016/s0735-1097(10)80145-7
55. Cerrone M, Colombi B, Santoro M, di Barletta MR, Scelsi M, Villani L, Napolitano C, Priori SG. Bidirectional ventricular tachycardia and fibrillation elicited in a knock-in mouse model carrier of a mutation in the cardiac ryanodine receptor. *Circ Res*. 2005;96:e77–e82. doi: 10.1161/01.RES.0000169067.51055.72
56. Zhou Q, Xiao J, Jiang D, Wang R, Vembaiyan K, Wang A, Smith CD, Xie C, Chen W, Zhang J, et al. Carvedilol and its new analogs suppress arrhythmogenic store overload-induced Ca^{2+} release. *Nat Med*. 2011;17:1003–1009. doi: 10.1038/nm.2406
57. Loaiza R, Benkusky NA, Powers PP, Hacker T, Noujaim S, Ackerman MJ, Jalife J, Valdivia HH. Heterogeneity of ryanodine receptor dysfunction in a mouse model of catecholaminergic polymorphic ventricular tachycardia. *Circ Res*. 2013;112:298–308. doi: 10.1161/CIRCRESAHA.112.274803
58. Song L, Alcalai R, Arad M, Wolf CM, Toka O, Conner DA, Berul CI, Eldar M, Seidman CE, Seidman JG. Calsequestrin 2 (CASQ2) mutations increase expression of calreticulin and ryanodine receptors, causing catecholaminergic polymorphic ventricular tachycardia. *J Clin Invest*. 2007;117:1814–1823. doi: 10.1172/JCI31080
59. Chen X, Weber C, Farrell ET, Alvarado FJ, Zhao YT, Gómez AM, Valdivia HH. Sorcin ablation plus β-adrenergic stimulation generate an arrhythmogenic substrate in mouse ventricular myocytes. *J Mol Cell Cardiol*. 2018;114:199–210. doi: 10.1016/j.yjmcc.2017.11.017
60. Tada M, Takeuchi A, Hashizume M, Kitamura K, Kano M. A highly sensitive fluorescent indicator dye for calcium imaging of neural activity in vitro and in vivo. *Eur J Neurosci*. 2014;39:1720–1728. doi: 10.1111/ejn.12476
61. Lock JT, Parker I, Smith IF. A comparison of fluorescent Ca^{2+} indicators for imaging local Ca^{2+} signals in cultured cells. *Cell Calcium*. 2015;58:638–648. doi: 10.1016/j.ceca.2015.10.003
62. Kapoor N, Tran A, Kang J, Zhang R, Philipson KD, Goldhaber JI. Regulation of calcium clock-mediated pacemaking by inositol-1,4,5-trisphosphate receptors in mouse sinoatrial nodal cells. *J Physiol*. 2015;593:2649–2663. doi: 10.1113/JP270082
63. Kanemaru K, Suzuki J, Taiko I, Iino M. Red fluorescent CEPIA indicators for visualization of Ca^{2+} dynamics in mitochondria. *Sci Rep*. 2020;10:2835. doi: 10.1038/s41598-020-59707-8
64. Nakamura T, Ogawa M, Kojima K, Takayanagi S, Ishihara S, Hattori K, Naguro I, Ichijo H. The mitochondrial Ca^{2+} uptake regulator, MICU1, is involved in cold stress-induced ferroptosis. *EMBO Rep*. 2021;22:e51532. doi: 10.15252/embr.202051532
65. Shannon TR, Ginsburg KS, Bers DM. Quantitative assessment of the SR Ca^{2+} leak-load relationship. *Circ Res*. 2002;91:594–600. doi: 10.1161/01.res.0000036914.12686.28
66. Shannon TR, Ginsburg KS, Bers DM. Potentiation of fractional sarcoplasmic reticulum calcium release by total and free intra-sarcoplasmic reticulum calcium concentration. *Biophys J*. 2000;78:334–343. doi: 10.1016/S0006-3495(00)76596-9
67. Saiki Y, Ikemoto N. Coordination between Ca^{2+} release and subsequent reuptake in the sarcoplasmic reticulum. *Biochemistry*. 1999;38:3112–3119. doi: 10.1021/bi982250m
68. Anderson ME, Brown JH, Bers DM. CaMKII in myocardial hypertrophy and heart failure. *J Mol Cell Cardiol*. 2011;51:468–473. doi: 10.1016/j.yjmcc.2011.01.012
69. Nolla-Colomer C, Casabella-Ramon S, Jimenez-Sabado V, Vallmitjana A, Tarifa C, Herraiz-Martínez A, Llach A, Tauron M, Montiel J, Cinca J, et al. β2-adrenergic stimulation potentiates spontaneous calcium release by increasing signal mass and co-activation of ryanodine receptor clusters. *Acta Physiol (Oxf)*. 2022;234:e13736. doi: 10.1111/apha.13736
70. Wei J, Guo W, Wang R, Paul Estillore J, Belke D, Chen YX, Vallmitjana A, Benitez R, Hove-Madsen L, Chen SRW. RyR2 serine-2030 PKA site governs Ca^{2+} release termination and Ca^{2+} alternans. *Circ Res*. 2023;132:e59–e77. doi: 10.1161/CIRCRESAHA.122.321177
71. Junqueira LC, Bignolas G, Brentani RR. Picrosirius staining plus polarization microscopy, a specific method for collagen detection in tissue sections. *Histochem J*. 1979;11:447–455. doi: 10.1007/BF01002772
72. Cuerrier CM, Chen YX, Tremblay D, Rayner K, McNulty M, Zhao X, Kennedy CR, de BelleRoche J, Pelling AE, O'Brien ER. Chronic over-expression of heat shock protein 27 attenuates atherogenesis and enhances plaque remodeling: a combined histological and mechanical assessment of aortic lesions. *PLoS One*. 2013;8:e55867. doi: 10.1371/journal.pone.0055867
73. Murali M, Turner SR, Belke DD, Cole WC, MacDonald JA. Smoothelin-like 1 knockout mice display sex-dependent alterations in blood flow and cardiac function. *Can J Physiol Pharmacol*. 2023;101:27–40. doi: 10.1139/cjpp-2022-0172
74. Chen B, Guo A, Gao Z, Wei S, Xie YP, Chen SR, Anderson ME, Song LS. In situ confocal imaging in intact heart reveals stress-induced Ca^{2+} release variability in a murine catecholaminergic polymorphic ventricular tachycardia model of type 2 ryanodine receptor(R4496C+/-) mutation. *Circ Arrhythm Electrophysiol*. 2012;5:841–849. doi: 10.1161/CIRCEP.111.969733
75. Bai Y, Jones PP, Guo J, Zhong X, Clark RB, Zhou Q, Wang R, Vallmitjana A, Benitez R, Hove-Madsen L, et al. Phospholamban knockout breaks arrhythmogenic Ca^{2+} waves and suppresses catecholaminergic polymorphic ventricular tachycardia in mice. *Circ Res*. 2013;113:517–526. doi: 10.1161/CIRCRESAHA.113.301678
76. Xiao J, Tian X, Jones PP, Bolstad J, Kong H, Wang R, Zhang L, Duff HJ, Gillis AM, Fleischer S, et al. Removal of FKBP12.6 does not alter the conductance and activation of the cardiac ryanodine receptor or the susceptibility to stress-induced ventricular arrhythmias. *J Biol Chem*. 2007;282:34828–34838. doi: 10.1074/jbc.M707423200
77. Zhong X, Sun B, Vallmitjana A, Mi T, Guo W, Ni M, Wang R, Guo A, Duff HJ, Gillis AM, et al. Suppression of ryanodine receptor function prolongs Ca^{2+} release refractoriness and promotes cardiac alternans in intact hearts. *Biochem J*. 2016;473:3951–3964. doi: 10.1042/BCJ20160606
78. Sikkel MB, Francis DP, Howard J, Gordon F, Rowlands C, Peters NS, Lyon AR, Harding SE, MacLeod KT. Hierarchical statistical techniques are necessary to draw reliable conclusions from analysis of isolated cardiomyocyte studies. *Cardiovasc Res*. 2017;113:1743–1752. doi: 10.1093/cvr/cvx151